




Article

Symmetry Constraints on Spin Order Transfer in Parahydrogen-Induced Polarization (PHIP)

 Andrey N. Pravdivtsev ^{1,*} , Danila A. Barskiy ^{2,3,*} , Jan-Bernd Hövener ¹ and Igor V. Koptyug ⁴ 

¹ Section Biomedical Imaging, Molecular Imaging North Competence Center (MOIN CC), Department of Radiology and Neuroradiology, University Medical Center Schleswig-Holstein (UKSH), Kiel University, Am Botanischen Garten 14, 24118 Kiel, Germany; jan.hoeverner@rad.uni-kiel.de

² Helmholtz-Institut Mainz, GSI Helmholtzzentrum für Schwerionenforschung, 55128 Mainz, Germany

³ Quantum, Atomic, and Neutron Physics (QUANTUM) Institute of Physics, Johannes Gutenberg University, Mainz, 55099 Mainz, Germany

⁴ International Tomography Center, SB RAS, 3A Institutskaya st., 630090 Novosibirsk, Russia; koptyug@tomo.nsc.ru

* Correspondence: andrey.pravdivtsev@rad.uni-kiel.de (A.N.P.); dbarskiy@uni-mainz.de (D.A.B.)

Abstract: It is well known that the association of parahydrogen (pH₂) with an unsaturated molecule or a transient metalorganic complex can enhance the intensity of NMR signals; the effect is known as parahydrogen-induced polarization (PHIP). During recent decades, numerous methods were proposed for converting pH₂-derived nuclear spin order to the observable magnetization of protons or other nuclei of interest, usually ¹³C or ¹⁵N. Here, we analyze the constraints imposed by the topological symmetry of the spin systems on the amplitude of transferred polarization. We find that in asymmetric systems, heteronuclei can be polarized to 100%. However, the amplitude drops to 75% in A₂BX systems and further to 50% in A₃B₂X systems. The latter case is of primary importance for biological applications of PHIP using sidearm hydrogenation (PHIP-SAH). If the polarization is transferred to the same type of nuclei, i.e., ¹H, symmetry constraints impose significant boundaries on the spin-order distribution. For AB, A₂B, A₃B, A₂B₂, AA'(AA') systems, the maximum average polarization for each spin is 100%, 50%, 33.3%, 25%, and 0, respectively, (where A and B (or A') came from pH₂). Remarkably, if the polarization of all spins in a molecule is summed up, the total polarization grows asymptotically with ~1.27√N and can exceed 2 in the absence of symmetry constraints (where N is the number of spins). We also discuss the effect of dipole–dipole-induced pH₂ spin-order distribution in heterogeneous catalysis or nematic liquid crystals. Practical examples from the literature illustrate our theoretical analysis.

Keywords: parahydrogen; polarization transfer; hyperpolarization; symmetry constraints; PHIP; PASADENA; ALTADENA; nuclear spin isomers; symmetry groups



Citation: Pravdivtsev, A.N.; Barskiy, D.A.; Hövener, J.-B.; Koptyug, I.V. Symmetry Constraints on Spin Order Transfer in Parahydrogen-Induced Polarization (PHIP). *Symmetry* **2022**, *14*, 530. <https://doi.org/10.3390/sym14030530>

Academic Editor: Gabriele Stevanato

Received: 13 December 2021

Accepted: 27 February 2022

Published: 4 March 2022

Publisher's Note: MDPI stays neutral with regard to jurisdictional claims in published maps and institutional affiliations.



Copyright: © 2022 by the authors. Licensee MDPI, Basel, Switzerland. This article is an open access article distributed under the terms and conditions of the Creative Commons Attribution (CC BY) license (<https://creativecommons.org/licenses/by/4.0/>).

1. Introduction

Parahydrogen-induced polarization (PHIP) is a cost-efficient and fast method to polarize nuclear spins [1]. PHIP exploits the symmetry of molecular dihydrogen that exists as two nuclear spin isomers: Parahydrogen (pH₂) and orthohydrogen (oH₂). The nuclear spin state of pH₂ is the singlet state, $|S\rangle = \frac{|\alpha\beta\rangle - |\beta\alpha\rangle}{\sqrt{2}}$, which is asymmetric under the exchange of the nuclear spins. The total wave function of the H₂ nuclei is antisymmetric under the exchange of two nuclei (two fermions), so the quantum numbers of the rotational states take even values [2]. oH₂ is represented by three nuclear spin states, $|T_0\rangle = \frac{|\alpha\beta\rangle + |\beta\alpha\rangle}{\sqrt{2}}$, $|T_+\rangle = |\alpha\alpha\rangle$, and $|T_-\rangle = |\beta\beta\rangle$. These three nuclear spin states are symmetric under spin exchange, hence necessitating odd rotational quantum numbers [2]. This selection is dictated by the generalized Pauli principle, which states that the total wave function of two protons (two fermions with spin- $\frac{1}{2}$) is antisymmetric upon permutation [2].

Note, however, that the hydrogen atom, consisting of a proton and an electron (i.e., two fermions), is a boson, hence the total wave function of H_2 is symmetric under the exchange of two atoms (further discussion below). Note that here we discuss the interplay between the symmetry of the nuclear spin states and symmetry of rotation–molecular spin states.

Thus, pH_2 takes the lowest rotational energy state, which is symmetric, and oH_2 takes the next rotational energy state, which is asymmetric. The gap between the lowest two rotational energy levels, i.e., pH_2 and oH_2 , is significant (170.5 K) and can be used to enrich the para-state: 50% pH_2 is obtained by cooling H_2 to liquid nitrogen temperatures [3] and 99% at about 25 K (e.g., using a two-stage Helium cryo-cooler or liquid Helium) [4,5]. Because pH_2 and oH_2 can be separated, they are also referred to as nuclear spin isomers (NSIM). Some other molecules also have NSIM, for instance, molecular deuterium [6], ethylene [7], and water [8].

The density matrix for an ensemble of molecules containing N spin- $\frac{1}{2}$ nuclei, where spins A and B originate from pH_2 , can be written as follows:

$$\hat{\rho}_S^{A,B} = \frac{\hat{1}^N}{2^N} - \frac{1}{2^{N-2}} (\hat{\mathbf{I}}^A \cdot \hat{\mathbf{I}}^B). \quad (1)$$

Here, $\hat{1}^N$ is the identity matrix, i.e., a $\{2^N \times 2^N\}$ matrix with ones on the diagonal.

The individual spin operators $\hat{I}_k^{A,B}$ in the dot product, $(\hat{\mathbf{I}}^A \cdot \hat{\mathbf{I}}^B) = \hat{I}_X^A \hat{I}_X^B + \hat{I}_Y^A \hat{I}_Y^B + \hat{I}_Z^A \hat{I}_Z^B$, are obtained using the Kronecker (direct) product \otimes of the corresponding Pauli matrices \hat{s}_k (with $k = X, Y$ or Z) and $N - 1$ of 2×2 identity matrices $\hat{1}^1$. Here, the numbering of the spins in the molecule is important. For example, for the first spin, the operator is constructed as

$$\hat{I}_k^1 = \frac{1}{2} \hat{s}_k \otimes \hat{1}^1 \dots \otimes \hat{1}^1. \quad (2)$$

There are two primary variants of PHIP: (a) Hydrogenative PHIP (Figure 1A), such as PASADENA (parahydrogen and synthesis allow dramatically enhanced nuclear alignment [9]) and ALTADENA (adiabatic longitudinal transport after dissociation engenders net alignment [10]), and (b) non-hydrogenative PHIP, or SABRE (signal amplification by reversible exchange [11], Figure 1B), where pH_2 and the substrate interact via a reversible exchange at a catalyst. Both methods have found applications at high ($\sim T$) [12], low ~ 1 mT [13], ultra-low ~ 1 μT [14,15], and zero fields [16]. To limit the scope of this paper, however, we focus our discussion on hydrogenative PHIP at high magnetic fields only. It should be noted that a similar analysis for four spin- $\frac{1}{2}$ SABRE systems was recently performed [17].

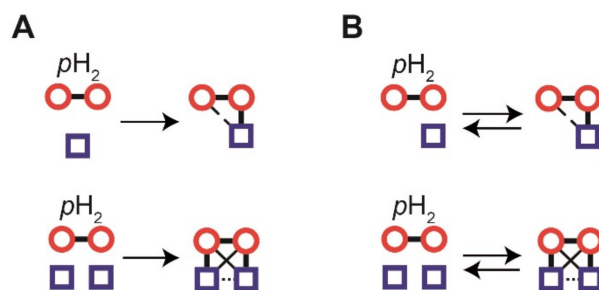


Figure 1. Schematic view of hydrogenative ((A), left) and non-hydrogenative ((B), right) PHIP for a 3-spin- $\frac{1}{2}$ system with asymmetric couplings (top) and a 4-spin- $\frac{1}{2}$ system with symmetric couplings (bottom). Here, we focus on hydrogenative PHIP in symmetric and asymmetric systems (A). The case of 4-spin- $\frac{1}{2}$ SABRE ((B), bottom) was considered by Levitt in a seminal paper [17]. Note that different lines represent different strengths of nuclear spin–spin interactions. pH_2 is represented by red circles, other spins or other reagents by blue squares, and J-couplings by thin, thick, and dashed lines.

For hydrogenative PHIP, the spin state of the molecule after pH₂ addition strongly depends on the coupling regime. Two spins $\hat{\mathbf{I}}^{\wedge A}$ and $\hat{\mathbf{I}}^{\wedge B}$ are considered strongly coupled when the difference of their Larmor precession frequencies, $\delta\nu_{AB} = |\nu_A^0 - \nu_B^0|$, is much smaller than their mutual indirect spin–spin coupling J_{AB} , i.e., $\delta\nu_{AB} \ll |J_{AB}|$. In the opposite case, the spins are weakly coupled [18]. The frequency $\nu_{A,B}^0 = \gamma_{A,B}B_0(1 + \delta_{A,B})/2\pi$ of spin $\hat{\mathbf{I}}^{\wedge A}$ or $\hat{\mathbf{I}}^{\wedge B}$ depends on the strength of the magnetic field B_0 , chemical shift $\delta_{A,B}$, and magnetogyric ratio $\gamma_{A,B}$.

In the PASADENA case, upon the addition of pH₂ to an asymmetric molecular environment at high fields, ¹H spins are weakly coupled. Since individual molecular hydrogenation events are distributed in time over the course of the hydrogenation reaction, the molecules evolve for different times, and the non-stationary X and Y coherences (Equation (1)) are lost. The singlet spin state $\hat{\rho}_S^{A,B}$ is averaged to the non-evolving stationary state, the so-called ZZ spin order [1]:

$$\hat{\rho}_{ZZ}^{A,B} = \frac{\hat{1}^N}{2^N} - \frac{1}{2^{N-2}} \hat{I}_Z^A \cdot \hat{I}_Z^B. \quad (3)$$

From now on, we will omit operator “hats”.

It is common to transfer pH₂-derived spin alignment to proton and X-nuclear magnetization (e.g., ¹³C, ¹⁵N, ¹⁹F) for use as an MRI contrast agent [19–21], monitoring of chemical and enzymatic reactions [7,22], or for analytical chemistry [23]. Many of such spin-order transformations are represented by unitary transformations of the density matrix:

$$\rho(t) = U(t, t_0)\rho(t_0)U(t, t_0)^\dagger, \quad (4)$$

where $\rho(t_0)$ is the density matrix at time t_0 , before the spin-order transfer (SOT), and $\rho(t)$ is the final density matrix, after the SOT. The unitary evolution operators $U(t, t_0)$, also known as propagators, can be found by solving the corresponding Liouville von-Neumann equation,

$$\frac{d}{dt}U(t, t_0) = -H(t)U(t, t_0) \quad (5)$$

for a time-dependent Hamiltonian $H(t)$ and the initial condition $U(t_0, t_0) = 1^N$.

In this work, we discuss the transformation of the singlet-state density matrix $\hat{\rho}_S^{A,B}$ and “PASADENA” density matrix $\hat{\rho}_{ZZ}^{A,B}$ to observable magnetization for various spin systems using general properties of unitary transformations [24,25] together with restrictions imposed by molecular symmetry [17].

2. Methods

2.1. Spin Operators and Observables

The general SOT from the initial spin state σ_{initial} to the desired target spin state σ_{target} under the action of the propagator U can be written as

$$U\sigma_{\text{initial}}U^\dagger = \sigma_{\text{final}} = \zeta\sigma_{\text{target}} + \sigma_{\text{rest}} \quad (6)$$

where σ_{final} is the final spin state, ζ is the amplitude of the target spin state σ_{target} , and σ_{rest} is the difference between σ_{final} and $\zeta\sigma_{\text{target}}$ that is not relevant for our considerations. We will use ρ for density matrices with the trace of one and σ for traceless spin operators (or traceless density matrices).

Since the propagator U is unitary, the transformation (6) implies boundaries on the parameter ζ . There is no general way to determine all possible final states σ_{final} for undefined U . However, it is possible to obtain boundary conditions for the amplitude $\zeta \in [\zeta_{\text{min}}, \zeta_{\text{max}}]$ and a given σ_{initial} and σ_{target} in general.

We define the operator of polarization of a single spin (e.g., A) in a molecule as

$$\sigma_P^A = \frac{1}{2^{N-1}} I_Z^A \quad (7)$$

and the operator of polarization of N spins-1/2 as

$$\sigma_P^N = \frac{1}{2^{N-1}} \sum_{k=1}^N I_Z^k. \quad (8)$$

Now it is straightforward to calculate a polarization (P) of one spin, or the average of many spins, using corresponding spin operators (7) and (8):

$$P = \frac{\text{Tr}(\rho(t) \cdot \sigma_P)}{\text{Tr}(\sigma_P \cdot \sigma_P)}. \quad (9)$$

Here, $\rho(t)$ is the density matrix of the system at the time of interest t .

In the same fashion, the amplitude ζ of the state σ_{target} for σ_{final} after SOT can be evaluated as:

$$\zeta = \frac{\text{Tr}(\sigma_{\text{final}} \cdot \sigma_{\text{target}})}{\text{Tr}(\sigma_{\text{target}} \cdot \sigma_{\text{target}})}. \quad (10)$$

We will use ζ in the following to report the maximum theoretically possible polarization ($\sigma_{\text{target}} = \sigma_P$).

We note that care should be taken when different initial states are analyzed. For example, consider a general operator in the form $\frac{\hat{1}^N}{2^N} + P\sigma_P^N$ that consists of two orthogonal operators $\frac{\hat{1}^N}{2^N}$ and σ_P^N (Equation (8)). Here, all diagonal elements of the unitary operator are $\frac{1}{2^N}$ and the largest element (its absolute value) of σ_P^N is equal to the maximum total spin of N spin-1/2 system, $N \cdot \frac{1}{2}$, times the normalization coefficient $\frac{1}{2^{N-1}}$, that is, $\frac{N}{2^N}$. Since the population of any individual state must be between 0 and 1, additional constraints are imposed on the allowed values of P : $0 \leq \frac{1}{2^N} \pm P \frac{N}{2^N} \leq 1$. One can see that to avoid non-negative populations, $|P| \leq \frac{1}{N}$ is needed. This means that for the system of two spins with net magnetization, the maximum average polarization per spin can only be 50%. However, if there are other components in the density matrix, larger values of P are possible. For example, the polarization of spins in $|T_+\rangle$ state is 100%; the corresponding density matrix is $\frac{\hat{1}^{N=2}}{4} + \sigma_P^N = 2 + I_Z^1 I_Z^2$ for $N = 2$.

2.2. No Symmetry Constraints

The boundaries for the amplitude ζ of the target state σ_{target} after SOT (Equation (6)) are [24]

$$\begin{aligned} \zeta_{\text{max}} &= \|\sigma_{\text{target}}\|^{-1} \cdot \left(\Lambda_{\text{initial}}^{\uparrow} \cdot \Lambda_{\text{target}}^{\uparrow} \right), \\ \zeta_{\text{min}} &= \|\sigma_{\text{target}}\|^{-1} \cdot \left(\Lambda_{\text{initial}}^{\uparrow} \cdot \Lambda_{\text{target}}^{\downarrow} \right), \\ \|\sigma_{\text{target}}\| &= \left(\Lambda_{\text{target}}^{\uparrow} \cdot \Lambda_{\text{target}}^{\uparrow} \right). \end{aligned} \quad (11)$$

Here, Λ_{initial} and Λ_{target} are the eigenvalues arranged in vectors for the operators σ_{initial} and σ_{target} . The arrows up (\uparrow) and down (\downarrow) indicate that these eigenvalues are sorted in an ascending or descending order. In general, $\zeta_{\text{min}} \leq \zeta \leq \zeta_{\text{max}}$.

These boundaries arise because we assume all transformations to be unitary, and the initial and final states are given by Hermitian operators [24]. Because σ_{initial} and σ_{target} are traceless operators, the boundary parameters often have the same absolute value: $\zeta_{\text{max}} = |\zeta_{\text{min}}|$ unless otherwise noted.

2.3. Symmetry Constraints (SC)

When a system has spin symmetry (i.e., groups of equivalent spins), only the states belonging to the same irreducible representations (Γ) of this group of symmetry G can be mixed by unitary transformations [17,24,25]. In this case, the boundary conditions can be found as:

$$\begin{aligned} \zeta_{\max}^{\text{SC}} &= \|\sigma_{\text{target}}\|^{-1} \sum_{\Gamma} \left(\Lambda_{\text{initial}}^{\uparrow, \Gamma} \cdot \Lambda_{\text{target}}^{\uparrow, \Gamma} \right), \\ \zeta_{\min}^{\text{SC}} &= \|\sigma_{\text{target}}\|^{-1} \sum_{\Gamma} \left(\Lambda_{\text{initial}}^{\uparrow, \Gamma} \cdot \Lambda_{\text{target}}^{\downarrow, \Gamma} \right). \end{aligned} \tag{12}$$

where $\Lambda_X^{\uparrow, \Gamma}$ are vectors of eigenvalues of the operator σ_X ($X = \text{initial or target}$) that correspond to eigenvectors belonging to the same Γ and sorted in an ascending (\uparrow) or descending (\downarrow) order.

The transformation amplitude ζ is bounded as $\zeta_{\min}^{\text{SC}} \leq \zeta \leq \zeta_{\max}^{\text{SC}}$.

2.4. Eigenvalues in the Case of SC

It is not trivial to define $\Lambda_X^{\uparrow, \Gamma}$ when SCs are present. To find the transformation of a density matrix σ into a *group-symmetrized* basis, one needs to construct a symmetry group-specific matrix Q from orthonormal basis vectors \vec{v} . Each vector \vec{v} must belong to only one irreducible representation Γ . Vectors \vec{v} are written vertically. Let us enumerate these vectors in such a way that all vectors from the same Γ stand next to each other: $Q = \begin{pmatrix} \vec{v}_1^{\rightarrow \Gamma 1} & \vec{v}_2^{\rightarrow \Gamma 1} & \vec{v}_3^{\rightarrow \Gamma 1} & \dots & \vec{v}_1^{\rightarrow \Gamma 2} & \dots & \vec{v}_m^{\rightarrow \Gamma k} \end{pmatrix}$. Then, the matrix of spin state σ (σ_{initial} or σ_{target}) in the new basis σ^Q can be found as

$$\sigma^Q = Q^{-1} \sigma Q. \tag{13}$$

There are three different situations for σ^Q :

1. **σ^Q is diagonal.** When the predefined basis of the group G coincides with the eigenstates of the operator σ , then σ^Q is diagonal with eigenvalues on the diagonal. All coherences (off-diagonal elements) are zero. To find $\Lambda^{\uparrow \text{or} \downarrow, \Gamma}$, one has only to sort and enumerate the eigenvalues inside each Γ :

$$\sigma^Q = Q^{-1} \sigma Q = \begin{pmatrix} \Lambda_1^{\Gamma 1} & 0 & \dots & 0 \\ 0 & \Lambda_2^{\Gamma 1} & \dots & 0 \\ \vdots & \vdots & \ddots & \vdots \\ 0 & 0 & \dots & \Lambda_m^{\Gamma k} \end{pmatrix}. \tag{14}$$

Here, $\Lambda_m^{\Gamma n}$ is an eigenvalue of σ and $\vec{v}_m^{\rightarrow \Gamma n}$ is its corresponding eigenvector belonging to irreducible representations Γn .

2. **σ^Q is Γ -block diagonal.** When σ^Q has coherences only inside the same irreducible representations Γ , then σ^Q is a Γ -block diagonal matrix

$$\sigma^Q = Q^{-1} \sigma Q = \begin{pmatrix} \Lambda^{\Gamma 1} & 0 & \dots & 0 \\ 0 & \Lambda^{\Gamma 2} & \dots & 0 \\ \vdots & \vdots & \ddots & \vdots \\ 0 & 0 & \dots & \Lambda^{\Gamma k} \end{pmatrix}. \tag{15}$$

Here, $\Lambda^{\Gamma m}$ are the corresponding blocks of irreducible representations Γm . Because all vectors from one Γ have the same symmetry, their superposition also has the same symmetry. It means that each block $\Lambda^{\Gamma m}$ should be additionally diagonalized, and resulting diagonal elements are corresponding eigenvalues $\Lambda_m^{\Gamma n}$.

3. σ^Q is not block diagonal. The most general case is when there are off-diagonal elements between different irreducible representations.

$$\sigma^Q = Q^{-1}\sigma Q = \begin{pmatrix} \Lambda^{\Gamma_1} & C_{\Gamma_1^2}^{\Gamma_1} & \cdots & C_{\Gamma_1^k}^{\Gamma_1} \\ C_{\Gamma_2}^{\Gamma_1} & \Lambda^{\Gamma_2} & & C_{\Gamma_2^k}^{\Gamma_1} \\ \vdots & & \ddots & \vdots \\ C_{\Gamma_k}^{\Gamma_1} & C_{\Gamma_k}^{\Gamma_2} & \cdots & \Lambda^{\Gamma_k} \end{pmatrix}. \quad (16)$$

In this situation, we will assume that the coherences $C_{\Gamma_n}^{\Gamma_m}$ are averaged to zero during the hydrogenation reaction due to magnetic field inhomogeneity and the different evolution of each hydrogenated molecule. When such off-diagonal elements are removed ($C_{\Gamma_n}^{\Gamma_m} = 0$), the σ^Q is “ Γ -block diagonal” and equivalent to Equation (15). Hence, the consequent diagonalization and analysis are equivalent and described in “case 2”.

In the following discussion, we use these three methods to find eigenvalues to evaluate ξ when SCs are imposed. A script is available in SI to evaluate ξ for a different number of spins, symmetry, initial, and target spin states (Matlab).

Below, we will discuss some specific cases and demonstrate the effect of symmetry on PHIP and spin order transfer.

2.5. Spin Systems Notations

We use a notation that is slightly different from Pople’s spin-system notation. The main idea is to distinguish the symmetries of the spin system. In addition, we fix X-spin to the target ^{13}C nucleus. Let us consider some examples.

First, for us, “ABC” stands for a system with three chemically nonequivalent spins, and only weak coupling is considered between spins. Second, “ A_2B ” stands for a system with two magnetically equivalent spins A_2 (strongly coupled) that are weakly coupled to B and have different chemical shifts with B. Third, according to Pople’s notation, $^{12}\text{C}_2$ -ethylene consists of four chemically and magnetically equivalent ^1H spins, hence the spin symmetry is A_4 . However, it does not reflect the permutation group symmetry of ethylene. Hence, we refer to the spin symmetry of $^{12}\text{C}_2$ -ethylene as $AA'(AA')$.

3. Results

Note that the polarization values reported in the following are the upper theoretical limits (as implied by the transformation mathematics).

3.1. Parahydrogen Spin-Order Transfer in a Two Spin-1/2 System

3.1.1. The Symmetry of AB and A_2 Systems

The simplest PHIP system consists of two spin-1/2 nuclei. If the protons of pH_2 after hydrogenation are magnetically and chemically nonequivalent (AB-system)—no symmetry constrains—the spins can be treated separately, and the appropriate basis would be the Zeeman basis:

$$S^{AB} = \{|\alpha\alpha\rangle, |\alpha\beta\rangle, |\beta\alpha\rangle, |\beta\beta\rangle\}. \quad (17)$$

When the protons are magnetically equivalent, the system is A_2 and there are restrictions on the choice of the basis. Here, singlet-triplet (S-T) states should be used:

$$S^{A_2} = \{|S\rangle, |T_+\rangle, |T_0\rangle, |T_-\rangle\}. \quad (18)$$

Among these two systems, only A_2 has nontrivial symmetry, which is C_2 . In Appendix A, we describe all relevant groups of symmetry. The transformation elements of the C_2 group are identity transformation E or null permutation “ $()$ ” and the permutation of two protons $\begin{pmatrix} 12 \\ 21 \end{pmatrix} = (21)$:

$$G^{12} = \{(), (21)\}. \quad (19)$$

The C_2 group (or G^{12}) has two irreducible representations: Even (gerade—"g") and odd (ungerade—"u"). The singlet state is the only member of the odd irreducible representation $\Gamma^u = B$, while three triplet states are the members of $\Gamma^g = A$. In terms of sets, it can be written as

$$\begin{aligned} S_A^{12} &= \{|T_+\rangle, |T_0\rangle, |T_-\rangle\}, \\ S_B^{12} &= \{|S\rangle\}. \end{aligned} \quad (20)$$

Tables of characters and decomposition of spin states into irreducible representations are given for A_2 , A_3 , and AA' (AA') systems in Appendix A.

3.1.2. pH_2 to Magnetization in AB Systems

Let us consider the transformation of $\sigma_{ZZ}^{A,B}$ spin order in an AB system (no symmetry constraints, Equation (11)) to magnetization (Equations (7) and (8)):

$$\sigma_{ZZ}^{A,B} = -I_Z^A \cdot I_Z^B \rightarrow \begin{cases} \frac{1}{2} I_Z^A, \text{ or } B, & |\xi| = 1, \\ \frac{1}{2} [I_Z^A + I_Z^B], & |\xi| = \frac{1}{2}, \\ \frac{1}{2} [I_Z^A - I_Z^B], & |\xi| = \frac{1}{2}. \end{cases} \quad (21)$$

This means that the PASADENA spin order ($\sigma_{ZZ}^{A,B}$) can be transferred to 100% polarization of one spin, or 50% polarization of each spin. In the latter case, the net magnetization can be 50% per spin or zero (21).

The examples of spin-order transfer (SOT) sequences for direct polarization transfers to one spin are Selective Excitation of Polarization using PASADENA (SEPP) [26] and adiabatic-passage spin order conversion (APSOC) [27–29]. SOT for polarization transfer to two spins include out of phase echo (OPE) [30], only parahydrogen spectroscopy (OPSY) [30,31], and APSOC [27–29].

3.1.3. pH_2 to Magnetization in A_2 Systems

The situation is different for two magnetically equivalent spins A^1 and A^2 in an A_2 spin system. Symmetry constraints do not allow spin order conversion of $\sigma_S^{A,B}$ into net magnetization:

$$\sigma_S^{A^1, A^2} = -(\mathbf{I}^{A^1} \cdot \mathbf{I}^{A^2}) \rightarrow \frac{1}{2} I_Z^{A^1} + \frac{1}{2} I_Z^{A^2}, \quad |\xi^{SC}| = 0 \quad (22)$$

The only way to transfer polarization is to break the symmetry ($A_2 \rightarrow AB$) that is happening e.g., during ALTADENA.

3.1.4. Limitation of the Method: ALTADENA Example

One of the first experiments that demonstrated spin order conversion of pH_2 was ALTADENA [10], using adiabatic magnetic field variation (AMFV). AMFV-induced spin order transfer in an AB two spin-1/2 system results in the following transformation of $\sigma_S^{A,B}$ [1]:

$$\sigma_S^{A,B} = -(\mathbf{I}^A \cdot \mathbf{I}^B) \xrightarrow{\text{AMFV}} -I_Z^A \cdot I_Z^B \pm \frac{1}{2} (I_Z^A - I_Z^B). \quad (23)$$

The sign (\pm) depends on the relative chemical shift difference and the sign of the J -coupling constant of the spins [1]. It follows that in ALTADENA, both spins acquire maximum polarization of 1 (see Equation (7)), but the total (net) polarization of the molecule is zero.

The Hamiltonian of an AB system H_{AB} is, in general, asymmetric (lacking permutation symmetry). However, at a zero field ($B_0 = 0$), it has the same permutation symmetry as the Hamiltonian of A_2 system H_{A_2} :

$$\begin{aligned}
 H_{AB}(B_0 \neq 0) &= -v_A^0 I_Z^A - v_B^0 I_Z^B + J_{AB}(\mathbf{I}^A \cdot \mathbf{I}^B), \\
 H_{AB}(B_0 = 0) &= J_{AB}(\mathbf{I}^A \cdot \mathbf{I}^B), \\
 H_{A_2}(B_0 \neq 0) &= -v_A^0 (I_Z^{A^1} + I_Z^{A^2}) + J_{A^1 A^2}(\mathbf{I}^{A^1} \cdot \mathbf{I}^{A^2}).
 \end{aligned}
 \tag{24}$$

This means that the initial and final symmetries of the Hamiltonian (and the spin system) are different and Equation (12) cannot be used for the estimation of ζ^{SC} (i.e., the symmetry changes during the experiment). We do not introduce a calculation method for such situations.

However, notice that the symmetry of the Hamiltonian (24) changes by introducing a magnetic field, while molecular symmetry does not change. This means that molecular symmetry does not have to coincide with the spin symmetry (or the symmetry of the nuclear spin Hamiltonian). The latter is essential for SOT, but molecular symmetry is essential for spin isomers (discussed below). Thus, there are at least three relevant symmetries: The Hamiltonian, interactions, and the spatial configuration of the molecule.

3.1.5. pH₂ on the Surface of a Solid

It was predicted that the spin order of pH₂ after chemisorption, i.e., interaction with a surface, could be transformed into net magnetization even when the two spins have the same chemical shifts [32,33]. Note that there are a minimum of two requirements for PHIP via chemisorption: (a) The pH₂ nascent protons have to be chemically nonequivalent, and (b) if they split, there is a non-zero chance to reunite again with preserved quantum coherences. The main reason for spin-order conversion is the difference in chemical shifts and the intramolecular dipole–dipole (DD) interaction, which is relevant on the surface. The Hamiltonian of such an AB system at a zero field is

$$H_{AB}^{DD}(B_0 = 0) = J_{AB}(\mathbf{I}^A \cdot \mathbf{I}^B) + d(\theta, \varphi)(3I_Z^A \cdot I_Z^B - (\mathbf{I}^A \cdot \mathbf{I}^B)). \tag{25}$$

As a result, the state of the dihydrogen after the chemisorption of pH₂ is expected to be a superposition of $\sigma_S^{A,B}$ and $\sigma_{ZZ}^{A,B}$ [33]:

$$\sigma_{S-DD}^{A,B} = -(P_{ZZ} - P_S)I_Z^A \cdot I_Z^B - P_S(\mathbf{I}^A \cdot \mathbf{I}^B). \tag{26}$$

where P_S and P_{ZZ} are the relative weight of the states σ_S and σ_{ZZ} . This result was predicted for two AB spins with the Hamiltonian H_{AB}^{DD} (Equation (26)) by averaging the pH₂-derived initial spin state, $\sigma_S^{A,B}$, over the hydrogenation period.

We showed before that it is impossible to transfer $\sigma_S^{A,B}$ to the total net magnetization of two spins in an A₂ system (Equation (22)). However, it is possible to transfer $\sigma_{ZZ}^{A,B}$:

$$\sigma_{ZZ}^{A,B} = -I_Z^A \cdot I_Z^B \rightarrow \frac{1}{2}[I_Z^A + I_Z^B], \quad |\zeta^{\text{SC}}| = 0.5, \tag{27}$$

even with symmetry constraints. Note that $|\zeta^{\text{SC}}| = |\zeta| = 0.5$ (compare Equations (21) and (26)).

However, one should bear in mind that the mere feasibility of such a transfer computed using the presented approach does not take into account whether or not there are interactions in the system that can be used for the observation of the resulting spin order. Using solid echo sequences, SOT from $\sigma_{ZZ}^{A,B}$ to $\sigma_P^{A,B}$ was predicted for chemisorbed pH₂ [32,33].

3.2. Transfer of pH₂ Spin Order to ¹H Magnetization in Multispin Systems

3.2.1. No Symmetry Constraints

Now we will consider the transfer of either $\sigma_{ZZ}^{A,B}$ or $\sigma_S^{A,B}$ spin orders into total spin magnetization, σ_P^N (Equation (8)), in asymmetric N spin-1/2 systems (Equation (11)).

The highest level of polarization (i.e., the average polarization across all coupled spins) is possible if the system is in a pure singlet state $\sigma_S^{A,B}$ rather than in $\sigma_{ZZ}^{A,B}$ (Figures 2–4 and Appendix B, Tables A6 and A7, and Appendix C for the corresponding analytical calculations for $N = 2, 3,$ and 4).

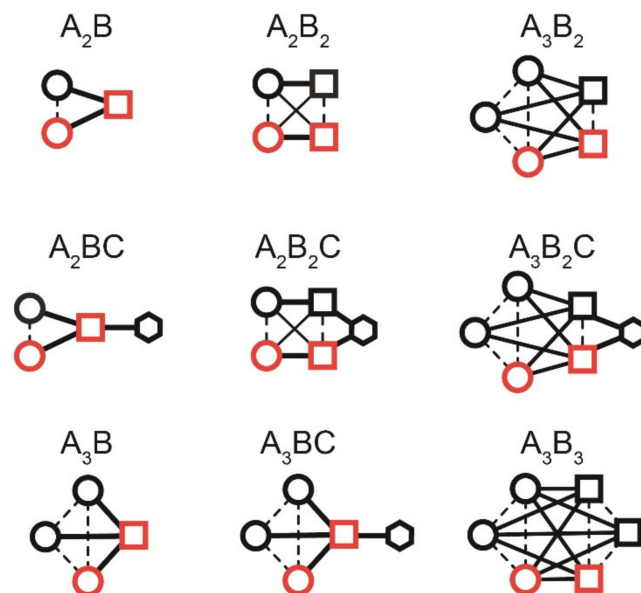


Figure 2. Spin topologies considered for simulating the effect of symmetry on the transformation of pD₂-derived spin order (red) into observable polarization. Red symbols indicate the pD₂-nascent spins, different lines indicate J -coupling constants, and circles, squares, hexagons are spins of the same type. Note that different lines represent different strengths of nuclear spin–spin interactions.

This situation is achieved when the S-T states are a (stationary) eigenbasis, i.e., when the J -couplings dominate the interactions. This can be achieved by adding pD₂ at low fields like in ALTADENA or via strong RF pulses suppressing chemical shift evolution at high fields [34]. Spin order transfer at the low field can be realized using SLIC pulses and was demonstrated for molecular systems with up to five nonequivalent spins [35].

Interestingly, the maximum achievable polarization per molecule increases up to 4 (i.e., the equivalent of 4 spins polarized to 100%) if the system approaches 10 spins and the initial density matrix is $\sigma_S^{A,B}$ (Figure 4); even higher polarizations are possible for a larger number of coupled spins (Appendix C).

Indeed, in an N -spin system where two spins are polarized with parahydrogen, $1/4$ of all states, 2^{N-2} , are equally populated. A unitary transformation can move that system into the state $|T_+\rangle \langle T_+| \otimes \hat{1}^{N-2}$, which has two spins with $P = 1$ (total polarization per molecule is then 2) and other spins are at equilibrium. Remarkably and nonintuitively, further unitary transformations can convert this into a state with higher angular momentum (or total polarization per molecule). Our calculations show that in the absence of symmetry constraints, the maximum of average spin polarization is approximately $1.27/\sqrt{N}$; this corresponds to a total polarization per molecule of $1.27\sqrt{N}$. For example, the sum of all polarizations in one molecule with $N = 500$ can reach ~ 29 (Appendix C).

We note that real systems always impose additional symmetry constraints, and calculated values of maximal polarization per molecule are significantly lower (see below).

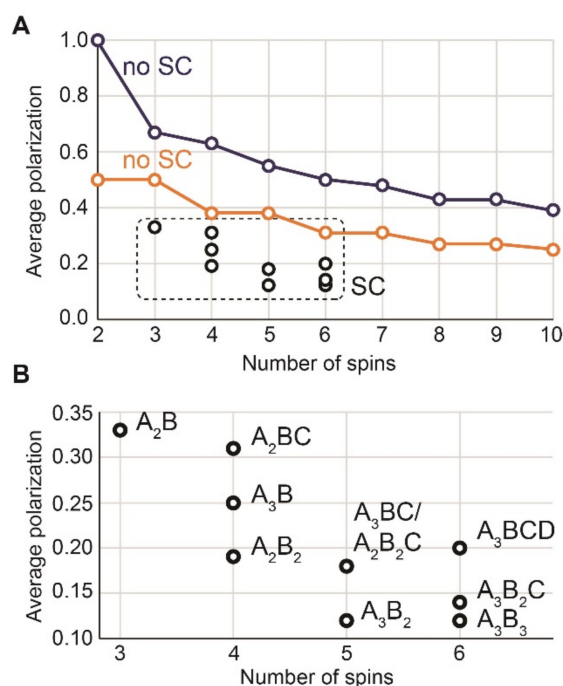


Figure 3. Average polarization per spin achieved theoretically by adding pH₂ to a precursor yielding a molecule with 2–10 spins with (black) and without (orange, blue) symmetry constraints (SC). In general, higher polarization can be achieved if there are no constraints (compare black with orange and blue) and if the initial density matrix is $\sigma_S^{A,B}$ (blue) rather than $\sigma_{ZZ}^{A,B}$ (orange, compare blue and orange in A). We assumed pH₂ to be added in positions A and B. The reported values are given in Tables A6 and A7 (Appendix B).

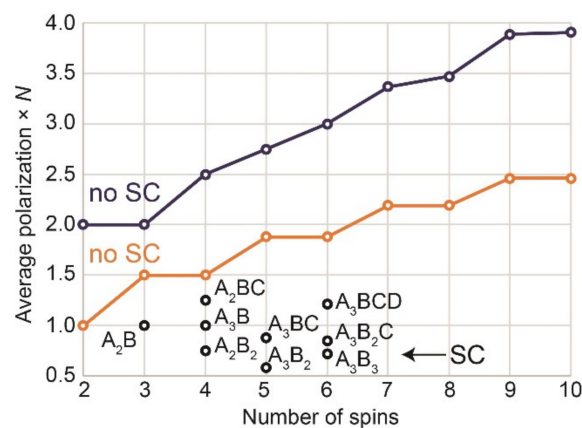


Figure 4. Average polarization per molecule—in units of one-spin-1/2 polarization—that can be achieved theoretically by adding pH₂ to a precursor yielding a molecule with 2–10 spins with (black, $\sigma_S^{A,B} \rightarrow \sigma_P^N$) and without symmetry constraints (SC) for $\sigma_S^{A,B} \rightarrow \sigma_P^N$ (blue) and $\sigma_{ZZ}^{A,B} \rightarrow \sigma_P^N$ (orange). If the polarization of all spins in one molecule is summed up, up to ~4 was obtained for large spin systems (blue). The reported values can be obtained from the average values given in Tables A6 and A7 (Appendix B) and calculations for $N = 2, 3$, and 4 exemplified in Appendix C.

3.2.2. With Symmetry Constraints

When a spin system topology has any permutation symmetries (Figure 2), the theoretically achievable proton polarization drops significantly. For example, in the A₃B₂C system of ethanol, the maximum average polarization is only 14.2% if pH₂ was added pairwise in positions A and B. If the symmetry constraints are relaxed so that six spins are

nonequivalent, the maximum achievable polarization increases to 31.2% for $\sigma_{\text{initial}} = \sigma_{ZZ}^{A,B}$ and 50% for $\sigma_{\text{initial}} = \sigma_S^{A,B}$, respectively (Figure 3).

Note that some similar systems were experimentally and theoretically studied in the related context of long-lived nuclear singlet spin states [36–38]. The process of spin order transfer discussed here is important for LLS because it gives the upper estimates for the maximum amplitude of the LLS conversion to magnetization.

3.2.3. Nuclear Spin Isomers of H₂ and Ethylene

Dihydrogen. We discuss nuclear spin isomers of molecules (NSIM) in more detail, starting with H₂. The molecular symmetry group of H₂ is D_{∞h}, while the permutation symmetry group of two spins is only C₂. The D_{∞h} symmetry includes an infinite number of symmetry elements and is a product of C₂ and C_∞ rotation groups, S_∞ rotation–reflection, and C_v groups. For the sake of simplicity, and to exemplify NSIM, let us consider the C₂ symmetry only. The four nuclear spin states (sp) of H₂ can be grouped in two sets A and B (Equation (20) and Appendix A): A^{sp} (3 states, oH₂) and B^{sp} (1 state, pH₂).

Ethylene. Ethylene is another example of a molecule with different NSIMs. Unlike H₂, however, the molecular symmetry group of ethylene is D_{2h}. Although the permutation symmetry group of spins is D₂ [39], it is helpful to use molecular symmetry to obtain a connection to corresponding rotational symmetries.

The permutation D₂ subgroup consists of one trivial and three nontrivial permutations that correspond to three orthogonal 180° rotations (Figure 5). In the D₂ symmetry group (see Appendix A), the 16 spin states (sp) of ethylene are grouped in four sets that correspond to A^{sp}, B₁^{sp}, B₂^{sp}, and B₃^{sp} symmetries; seven states for the A-symmetry set and three states for each of the B-symmetry sets.

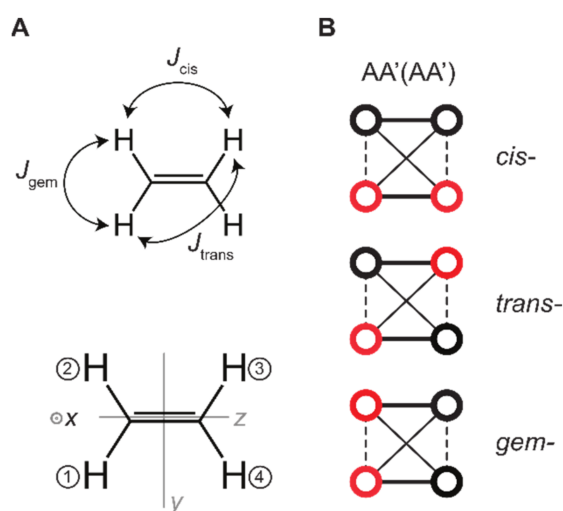


Figure 5. Interactions and symmetry axis of ethylene. (A) Ethylene structure and nuclear spin–spin couplings (J -couplings, top), the numbering of the atomic positions, and the cartesian axis x , y , z . (B) Graphs corresponding to the spin system AA'(AA') where pH₂ was added at cis-, trans-, or geminal positions (red circles). Different lines correspond to different values of spin–spin interactions.

The D_{2h} symmetry group includes additional inversion operation (*i*) and its combinations with the above-mentioned 180° rotations. In this case, the decomposition of 16 spin states also results in four groups with additional symmetry indices: A_g^{sp} (seven states), B_{1u}^{sp} (three states), B_{2u}^{sp} (three states), and B_{3g}^{sp} (three states). Seven states of A_g^{sp} symmetry include five states with total spin 2 (A_{g,2}^{sp}) and two states with total spin 0 (A_{g,01}^{sp} and A_{g,02}^{sp}). Each B group corresponds to three spin states of the same symmetry with the total spin 1.

The parity of spin states is even, and so is the parity of these four groups of symmetry. The rotational wavefunctions of ethylene are all of g symmetry, which leaves only four rotational (rot) symmetries, A_g^{rot} , B_{1g}^{rot} , B_{2g}^{rot} , and B_{3g}^{rot} .

The total (rotational and nuclear spin) wavefunction should have A-symmetry (either A_g or A_u), therefore there are four allowed combinations for ethylene: $A_g^{\text{rot}}A_g^{\text{sp}}$, $B_{1g}^{\text{rot}}B_{1u}^{\text{sp}}$, $B_{2g}^{\text{rot}}B_{2u}^{\text{sp}}$, $B_{3g}^{\text{rot}}B_{3g}^{\text{sp}}$.

We discuss the ethylene case in detail because it gives very good insight into the problem of polarization transfer between states of different symmetries.

Upon NSIM interconversion, the associated energy changes are much larger than what is normally induced in NMR by RF pulses. An NSIM interconversion inevitably changes both rotational and spin states of ethylene. This is in strong contrast to non-symmetric molecules where the energy of spin flips is comparable to the strength of nuclear spin interactions. The large gap between H_2 rotational energies helps to enrich the pH_2 state at low temperatures and is responsible for its long lifetime [3,5].

Some of the states belonging to different NSIMs of polyatomic molecules may have similar energies (in contrast to H_2 for which this is impossible). Such gateways are the basis of the quantum relaxation theory of NSIM interconversion [40]. For instance [41], for the B_{1g}^{rot} ($J = 23$) B_{1u}^{sp} and B_{2g}^{rot} ($J = 21$) B_{1g}^{sp} states of ethylene (where J is a rotational quantum number), the energy gap is “only” 46 MHz, i.e., within the reach of dipolar couplings. However, the energy of these states is 900 cm^{-1} (1300 K) above the ground state of ethylene; therefore, their thermal population is low and the NSIM interconversion is also relatively slow despite efficient mixing of these states by the dipole–dipole interaction.

Unlike in H_2 (with C_2 symmetry), in ethylene, it seems possible to transfer singlet state and ZZ spin order into magnetization:

$$\begin{aligned}\sigma_S^{\text{Am,An}} &= -\frac{1}{4}\mathbf{I}^{\text{Am}}\cdot\mathbf{I}^{\text{An}} \rightarrow \frac{1}{8}\left(I_Z^{\text{A1}} + I_Z^{\text{A2}} + I_Z^{\text{A3}} + I_Z^{\text{A4}}\right) \\ \sigma_{ZZ}^{\text{Am,An}} &= -\frac{1}{4}\mathbf{I}_Z^{\text{Am}}\cdot\mathbf{I}_Z^{\text{An}} \rightarrow \frac{1}{8}\left(I_Z^{\text{A1}} + I_Z^{\text{A2}} + I_Z^{\text{A3}} + I_Z^{\text{A4}}\right)\end{aligned}\quad (28)$$

with Am and An being one of four protons. Using the ethylene J -coupling constants to set the basis of spin states (Appendix A and ref [7], $J_g = 1.07 \text{ Hz}$, $J_c = 11.47 \text{ Hz}$, and $J_t = 17.78 \text{ Hz}$ [42]), the following values were obtained for different hydrogenation sites: $|\zeta_{S,cis}^{\text{SC}}| = |\zeta_{S,trans}^{\text{SC}}| = |\zeta_{S,gem}^{\text{SC}}| = 0.2$ and $|\zeta_{ZZ,cis}^{\text{SC}}| = |\zeta_{ZZ,trans}^{\text{SC}}| = |\zeta_{ZZ,gem}^{\text{SC}}| = 0.225$. According to Figure 5, here cis corresponds to protons 1 and 4 (or 2 and 3), trans to 1 and 3 (or 2 and 4), and gem to 1 and 2 (or 3 and 4). Note that using other simulations or isotope-labeling other (but similar) values were obtained and can be used [43]: $J_g = 2.23\text{--}2.39 \text{ Hz}$, $J_c = 11.62\text{--}11.66 \text{ Hz}$ and $J_t = 18.99\text{--}19.03 \text{ Hz}$; [44]: $J_g = 2.5 \text{ Hz}$, $J_c = 11.6 \text{ Hz}$ and $J_t = 19.1 \text{ Hz}$. However, because the constants were of the same order, we did not compare the spin order transfer for different J -coupling values.

It may come as a surprise that the efficient transfer of singlet spin order to polarization is feasible in a highly symmetric system like ethylene. So far, this transfer was demonstrated only in aligned media (nematic liquid crystals), where dipole–dipole spin–spin interactions remain, and the Hamiltonian of the system resembles H_{AB}^{DD} (Equation (25)). For such a Hamiltonian as discussed above, instead of pure $\sigma_S^{\text{Am,An}}$, a mixture of $\sigma_S^{\text{Am,An}}$ and $\sigma_{ZZ}^{\text{Am,An}}$ should be considered and $\sigma_{ZZ}^{\text{Am,An}}$ spin order is observable in NMR.

Normally, the transition between two states with spin 0 that are represented by $A_{g,01}^{\text{sp}}$ or 2 and $A_{g,2}^{\text{sp}}$ symmetries cannot be observed by NMR. However, the theory applied here still allows the transfer of spin order to polarization. Let us take a closer look and determine why this is possible.

After hydrogenation with pH_2 , six states with B-symmetry and two singlets of A_g symmetry is populated under each hydrogenation scenario (Table 1). The average polarization that we considered in Equation (28) depends on the populations of all symmetry states and is not straightforward to analyze. However, let us instead consider the state

$|2, 2\rangle = |\alpha\alpha\alpha\alpha\rangle$ with the maximum for the system value of spin and spin projection of 2; one of five states of A_g^{SP} symmetry. It means that if there is a way to transfer polarization from one of two $|0, 0\rangle$ spin states ($A_{g,0_1}^{SP}$ or $A_{g,0_2}^{SP}$) to the $|2, 2\rangle$ state (both have the same A_g^{SP} symmetry), ethylene hyperpolarization will be revealed. Now the question of how to achieve this remains, and if any existing spin order transfer methods, e.g., spin-lock-induced crossing (SLIC) [45], adiabatic passage spin order conversion (APSOC) [29], or magnetic field cycling (MFC) [46], are suitable. This analysis goes beyond the scope of this paper and will be considered elsewhere.

Table 1. Relative populations of spin symmetries in ethylene after addition of pH_2 in geminal (gem), cis, and trans position. Note that there are also coherences between $A_{g,0_1}^{SP}$ and $A_{g,0_2}^{SP}$ states, and between the two respective populated B-symmetries (e.g., B_{2u}^{SP} and B_{3g}^{SP} in case of pos. = gem).

Pos.	$A_{g,2}^{SP}$	$A_{g,0_1}^{SP}$	$A_{g,0_2}^{SP}$	B_{1u}^{SP}	B_{2u}^{SP}	B_{3g}^{SP}
gem	0	0.2409	0.009	0	1/8	1/8
cis	0	0.1075	0.1425	1/8	0	1/8
trans	0	0.0266	0.2234	1/8	1/8	0

3.3. PHIP-SAH and the Transfer of pH_2 Spin Order to the Magnetization of X-Nuclei

3.3.1. PHIP-SAH

Polarization transfer from pH_2 to X-nuclei also attracts significant attention in the context of hyperpolarized MRI applications. The lack of background signal and extended lifetime of polarization (compared to 1H) makes hyperpolarized MRI of X-nuclei highly interesting for biomedical applications, spearheaded by hyperpolarized MRI of xenon and ^{13}C -pyruvate [19,47–50].

PHIP by sidearm hydrogenation (PHIP-SAH) [51,52] (Figure 6) attracted significant attention because it allowed the polarization of acetate and pyruvate—the most commonly used contrast agents for hyperpolarized in vivo MRI [53,54].

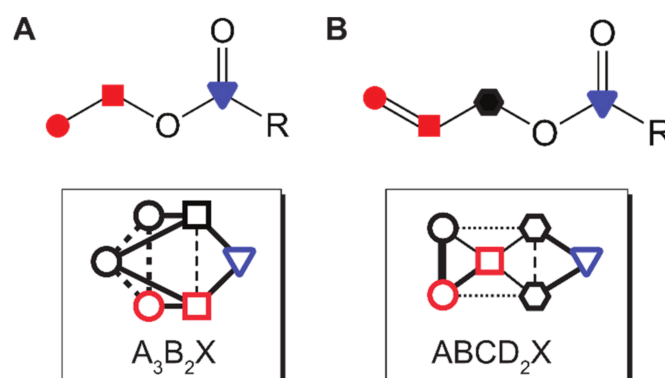


Figure 6. Molecular structures (top) and spin topologies (bottom) of ethyl (A) and allyl (B) esters of carboxylic acids—products of PHIP-SAH. Different lines (bottom) represent different spin–spin interaction values.

3.3.2. No Symmetry Constraints

We considered the transfer of $\sigma_S^{A,B}$ and $\sigma_{ZZ}^{A,B}$ to X-nuclear polarization (σ_P^X) without symmetry constraints (Table 2). In both cases, 100% polarization can be achieved: $|\zeta| = 1$. This, for example, was predicted for the hydrogenation of perdeuterated 1- ^{13}C -vinyl-acetate- d_6 [12]. More than 50% polarization was achieved on ^{13}C in the system consisting of three nonequivalent spin-1/2 and six spin-1 nuclei (2H). The direct loss of polarization is due to S- T_0 mixing of pH_2 -derived hydrogens at the catalyst and relaxation during hydrogenation [55].

Table 2. Polarization transfer from pH₂ ($\sigma_S^{A,B}$) to an X nucleus (σ_P^X). One hydrogen of pH₂ is in A, the other is in B position.

Type of the System	ζ_{\max} from $\sigma_S^{A,B} = \zeta \sigma_P^X + \sigma_{\text{rest}}$	Examples of Molecules, R = Acetate, Pyruvate
ABX, ABCX, ABCDX, ABCDEX, ... ABCD ₂ X	1	1- ¹³ C-vinyl-R
		1- ¹³ C-allyl-R
AA'BB'X	1	1- ¹³ C-ethylene
A ₂ BX	3/4	
A ₂ BC ₂ X	3/4	
A ₃ BX	2/3	
A ₂ B ₂ X	9/16	
A ₃ B ₂ X	1/2	1- ¹³ C-ethyl-R
A ₃ B ₂ C ₂ X	1/2	1- ¹³ C-propyl-R

3.3.3. Symmetry Constraints

If some other (i.e., non-nascent pH₂) protons possess any symmetry, 100% polarization transfer can still be achieved on X (theoretically). This situation is realized e.g., in 1-¹³C-allyl-pyruvate, an ABCD₂X system.

If one of the pH₂-nascent protons ends up in a symmetric site of the product, the maximum polarization that can be transferred to X is reduced to 75% for A₂BX ($|\zeta^{\text{SC}}| = 3/4$) and 66.(6)% for A₃BX ($|\zeta^{\text{SC}}| = 2/3$). Again, the number of the “other” protons and their symmetry does not play a role.

If both pH₂ spins bind to two different symmetric spin sites, such as A₃B₂X, A₃B₂C₂X, the maximum polarization that can be transferred to X is further reduced to 50% ($|\zeta^{\text{SC}}| = 0.5$). This situation is found, for example, in ethyl- and propyl pyruvate.

In the literature, ¹³C-polarization about 20% was reported on ethyl pyruvate. Here, pH₂ was added to vinyl pyruvate at a high field and spin order was transferred to ¹³C using INEPT [56]. About 20–35% ¹³C-polarization was reported in a similar experiment, where pH₂ was added at a low field and the detection took place at the high field after magnetic field variation [46,57]. However, one should remember that, as with the ALTADENA discussed above, the Hamiltonian of the system changes during the magnetic field variation.

The other interesting case, however exotic for PHIP, is the transfer of pH₂ spin order in an A₃X system if two of the A spins are in the singlet state ($|\zeta^{\text{SC}}| = 0$ for $\sigma_S^{A_i, A_j} \rightarrow \sigma_P^X$). If they are in the “reduced” singlet state σ_{ZZ} , however, the transfer is possible ($|\zeta^{\text{SC}}| = 1/3$ for $\sigma_{ZZ}^{A_i, A_j} \rightarrow \sigma_P^X$). For example, as we discussed before, pH₂-derived spin order after chemisorption is partially in the ZZ state.

3.3.4. Double Hydrogenation

Now we turn to the following question: Is it beneficial to add two pH₂ molecules to one target? For example, 1-¹³C-ethynyl pyruvate is transformed into 1-¹³C-ethyl pyruvate, an A₃B₂X system, by double hydrogenation (addition of two pH₂ molecules). Likewise, 1-¹³C-propargyl pyruvate becomes 1-¹³C propyl pyruvate, an A₃B₂C₂X system, upon the addition of two pH₂ (pH₂ is added to A and B in both cases).

Let us assume that the hydrogenation reaction is so fast that only the $|SS\rangle \langle SS|$ spin state is populated, which can be written as

$$\sigma_{S|S}^{A1, B1|A2, B2} = -\frac{1}{2^{N-2}} (\mathbf{I}^{A1} \cdot \mathbf{I}^{B1}) - \frac{1}{2^{N-2}} (\mathbf{I}^{A2} \cdot \mathbf{I}^{B2}) + \frac{1}{2^{N-4}} (\mathbf{I}^{A1} \cdot \mathbf{I}^{B1}) (\mathbf{I}^{A2} \cdot \mathbf{I}^{B2}) \quad (29)$$

The theoretically maximum transfer from $\sigma_{S|S}^{A_1, B_1|A_2, B_2}$ to X-nuclear polarization in A_3B_2X and $A_3B_2C_2X$ systems is $|\zeta^{SC}| = 1/4$, which is 2 times lower than for the single hydrogenation. Note that it is also system-specific, e.g., for the A_2B_2X system double hydrogenation results in $|\zeta^{SC}| = 3/4$, while $|\zeta^{SC}| = 9/16$ is the maximum predicted for single hydrogenation (Table 2).

In reality, however, there will be a finite time between the first and second hydrogenation, such that the system will start to evolve. As a result, the final state will be different than $|SS\rangle \langle SS|$ and the polarization of X nucleus will also be different.

The situation is similar for multiple hydrogenations in different positions, for example, in trivinyl orthoacetate [58]. If we simplify the product to two ethyl groups, the system becomes $(A_3B_2)(A_3B_2)'X$, where one pH_2 is part of the A_3B_2 subsystem and the other is part of $(A_3B_2)'$ subsystem. In this case, polarization transfer amplitude $|\zeta^{SC}| = 5/16$ was predicted, while for single hydrogenation (yielding an A_3B_2X system), it was $|\zeta^{SC}| = 1/2$.

We did not find instantaneous double hydrogenation beneficial for spin order transfer to X-nuclei, which may be different for slow and stepwise double hydrogenation.

3.4. Examples of Isotopic and Chemical Symmetry Breaking

3.4.1. Ethylene

Ethylene produced by adding pH_2 to acetylene in an isotropic environment does not demonstrate any enhanced observable magnetization. The spin state of pH_2 should be converted into the ZZ state instead: This was demonstrated after the hydrogenation and subsequent dissolution of ethylene in a liquid crystal [7]. However, one can imagine doing it in a different order. First, generate the ZZ-state of pH_2 -derived H_2 , which was estimated for a solid catalyst [32,33]. Second, hydrogenate acetylene using this H_2 .

In general, the pH_2 -derived protons are observed only when they are attached to chemically or magnetically inequivalent sites that for ethylene can be achieved in at least two ways:

- The two pairs of hydrogens in ethylene can be made magnetically nonequivalent by ^{13}C labeling. In the case of a single-sided ^{13}C labeling system, symmetry drops down to C_2 and polarization transfer is possible to 1H or ^{13}C nuclei. In addition, the chemical shifts of two gem pairs of protons are different.
- The other way to break the ethylene symmetry is a chemical reaction. So, polarized ethylene gas bubbled through a CCl_4 solution of perfluoro(para-tolylsulfenyl) chloride (PTSC) yields an asymmetric PTSC/ethylene adduct [7]. As a result, a normal PASADENA spectrum can be obtained.

3.4.2. Fumarate and Maleate

Fumarate and maleate are two metabolites with symmetry-imposed spin order transfer restrictions; the solutions are also the same. The symmetry can be broken by ^{13}C labeling [59,60] or as a result of a chemical reaction: "hyperpolarized" fumarate was converted by fumarase to asymmetric malate revealing itself in the PASADENA spectrum [61].

Dimethyl ether of maleate (and fumarate, another popular PHIP molecule) has C_s symmetry. However, pH_2 -derived protons are magnetically inequivalent because of the interaction with two CH_3 groups, and the spin order of pH_2 can be accessed with RF pulses [59] or magnetic field variation [37].

4. Discussion

We considered several cases of polarization transfer from pH_2 to proton and X nuclei magnetization using the methods introduced in refs. [17,24,25] (see Supplementary Materials). The approach used here helps to provide some general answers to several nonintuitive questions. However, a few situations remain unclear and may indicate some limitations of the presented theory. Namely:

Q1. How do we estimate maximum polarization transfer from a state that is not diagonal in the basis of the system's symmetry?

Q2. How do we estimate polarization transfer in systems that experience symmetry change during the polarization transfer, e.g., $A_2 \rightarrow AB$ during magnetic field variation in the ALTADENA experiment? Is there a general solution for an N -spin system?

Discussion of Q1. This situation corresponds to the third case of σ^Q -diagonalization (Equation (16)) as described in *methods*. For example, in an A_2BX system, the basis consists of the functions $|Mkl\rangle$ where $|M\rangle$ is one of S-T basis functions and $|k\rangle, |l\rangle$ are spin up and down, $|\alpha\rangle$ and $|\beta\rangle$. On this basis, $\sigma_S^{A_1,B}$ is not diagonal. Instead, projecting this state on the symmetry basis results in $\frac{1}{2}[\sigma_{ZZ}^{A_1,B} + \sigma_{ZZ}^{A_2,B}]$, meaning that we lose part of the initial spin order and potentially underestimate the level of polarization transfer.

Discussion of Q2. This problem was discussed in the context of ALTADENA, but it is also very important for magnetic field variation e.g., in PHIP-SAH. Let us consider a simple ABX system. At low fields, when the proton chemical shift difference can be neglected, the ABX system becomes equivalent to an A_2X system meaning that for protons, an S-T basis is more appropriate at low fields. $\sigma_S^{A,B}$ is the initial state of the system after pH_2 addition ($\sigma_{\text{initial}} = \sigma_S^{A,B}$). Then, we increase the field slowly so that the system changes from A_2X to ABX and the basis changes from S-T to Zeeman. This means that the symmetry basis of the system before and after (and during) the transformation is different. The theory presented here cannot be applied.

Although in three-spin systems, we can still reach 100% X nuclear polarization, we again could underestimate the efficiency of polarization transfer in more complex systems.

It seems as though the methodology used here for the static high magnetic field can be translated to low fields (and zero fields). However, the basis will be system-symmetry-specific and, in addition, will depend on the J -coupling network.

Assessing the validity of this approach is not straightforward. To date, however, experimental results have not contradicted the calculated results presented here.

5. Conclusions

The mathematical framework presented here allows for determining an upper limit for the polarization transfer from pH_2 to X-nuclei or other protons with an emphasis on the effect of molecular spin symmetry. Solutions were presented for the most current experimental situations, although more complex cases remain unaddressed. This method may serve as a first check to estimate if and how much polarization transfer is possible in a given situation. Naturally, identifying and optimizing a dedicated transfer strategy is the next essential step, which is not addressed here.

Supplementary Materials: The following supporting information can be downloaded at: <https://www.mdpi.com/article/10.3390/sym14030530/s1>. All used Matlab scripts together with MOIN spin library [62] (.zip) are available online.

Author Contributions: A.N.P., conceptualization and software; D.A.B. and J.-B.H. visualization; A.N.P. and D.A.B., original draft; A.N.P., D.A.B. and I.V.K., investigation. All authors, review and editing and funding acquisition. All authors have read and agreed to the published version of the manuscript.

Funding: We acknowledge funding from the German Federal Ministry of Education and Research (BMBF) within the framework of the e:Med research and funding concept (01ZX1915C), DFG (PR 1868/3-1, HO-4602/2-2, HO-4602/3, GRK2154-2019, EXC2167, FOR5042, SFB1479, TRR287), Kiel University and the Faculty of Medicine. MOIN CC was founded by a grant from the European Regional Development Fund (ERDF) and the Zukunftsprogramm Wirtschaft of Schleswig-Holstein (Project no. 122-09-053). DAB acknowledges support from the Alexander von Humboldt Foundation in the framework of the Sofja Kovalevskaja Award. I.V.K. acknowledges the Russian Ministry of Science and Higher Education (grant no. 075-15-2020-779) for financial support.

Institutional Review Board Statement: Not applicable.

Informed Consent Statement: Not applicable.

Data Availability Statement: All data and software obtained and used are available with the paper on [mdpi.com](https://www.mdpi.com).

Acknowledgments: We are grateful to Dmitry Budker for the discussion and editing of the manuscript. We are particularly thankful for the insightful comments from Warren S. Warren regarding large polarization obtained in multi-spin systems without symmetry constraints.

Conflicts of Interest: The authors declare no conflict of interest.

Appendix A

Appendix A.1. A2 Two Spin-1/2 System, C2 Group

The number of states is $2^2 = 4$.

The basis for two equivalent spins can be divided into two groups with a total spin I^{tot} of 1 (three states) and 0 (one state), also known as the singlet–triplet (S-T) basis. This can be derived formally by finding eigenfunctions and eigenvalues (λ) of the cyclic permutation operator $\begin{pmatrix} 1 & 2 \\ 2 & 1 \end{pmatrix} = (21)$. The C_2 permutation group of the A_2 system consists of two permutations, $\{(),(21)\}$. In the matrix form, it is written in the Zeeman basis ($|\alpha\alpha\rangle, |\alpha\beta\rangle, |\beta\alpha\rangle, |\beta\beta\rangle$):

$$\begin{aligned} () = E &= \begin{pmatrix} 1 & 0 & 0 & 0 \\ 0 & 1 & 0 & 0 \\ 0 & 0 & 1 & 0 \\ 0 & 0 & 0 & 1 \end{pmatrix}, \\ (21) = C_2 &= \begin{pmatrix} 1 & 0 & 0 & 0 \\ 0 & 0 & 1 & 0 \\ 0 & 1 & 0 & 0 \\ 0 & 0 & 0 & 1 \end{pmatrix}. \end{aligned} \tag{A1}$$

Eigenvalues of C_2 are given in superscript to the corresponding wavefunctions:

$$\begin{aligned} \lambda = 1, \text{ group 1} &\in A \\ |1, +1\rangle^1 &= |T_+\rangle = |\alpha\alpha\rangle, \\ |1, 0\rangle^1 &= |T_0\rangle = \frac{|\alpha\beta\rangle + |\beta\alpha\rangle}{\sqrt{2}}, \\ |1, -1\rangle^1 &= |T_-\rangle = |\beta\beta\rangle, \\ \lambda = -1, \text{ group 2} &\in B \\ |0, 0\rangle^{-1} &= |S_0\rangle = \frac{|\alpha\beta\rangle - |\beta\alpha\rangle}{\sqrt{2}}. \end{aligned} \tag{A2}$$

We indicate spin states by the total spin I^{tot} and its projection I_Z^{tot} as $|I^{\text{tot}}, I_Z^{\text{tot}}\rangle^\lambda$ and/or by using the Zeeman basis, $|\alpha\rangle$ and $|\beta\rangle$.

Table A1. Table of characters for A_2 two spin-1/2 system (C_2 group).

	E	C_2
A	1	1
B	1	-1
SpinRep = 3A + B	4	2

Therefore, there are three symmetric states and one asymmetric state with respect to (21) permutation (or rotation about 180 degrees, C_2). It follows from both Equation (A1) and Table A1. Therefore, the basis for A_2 two spin-1/2 system consists of two sets (S) with multiplicity of 3 and 1 (SpinRep = 3A + B):

$$\begin{aligned} S_A^{12} &= \{|T_+\rangle, |T_0\rangle, |T_-\rangle\}, \\ S_B^{12} &= \{|S_0\rangle\}. \end{aligned} \tag{A3}$$

To calculate characters for spin permutations (SpinRep) in Table A1, one can (i) write a matrix of permutation and (ii) calculate the trace. For an identity transformation, $() = E$, and for N spin-1/2, character is

$$\chi_{\text{SpinRep}}(E) = \text{Tr}(E) = 2^N. \tag{A4}$$

Analogously (Equation (A1)) $\chi_{\text{SpinRep}}(C_2) = \text{Tr}(C_2) = 2$.

For any character X of a representation $T = \oplus_i T_i$ which is a superposition of irreducible representations of the same group, the multiplicity n_k of the irreducible representation T_i is given by

$$n_k = \frac{1}{\Omega_G} \sum_g X(g)^* \chi_k(g). \tag{A5}$$

Here “*” is a complex conjugate, $\Omega_G = \sum_g \chi_k(g)^* \chi_k(g)$ and χ_k is a character of an irreducible representation Γ_k . Equation (A5) is useful to decompose the SpinRep line into a sum of characters for irreducible representations. So, for the A_2 system SpinRep = 3A + B.

Appendix A.2. A3 Three Spin-1/2 System, C3 Group

The number of states is $2^3 = 8$.

The basis of three equivalent spins can be grouped into three groups with a total spin I^{tot} of 3/2 (four states), 1/2 (two states), and 1/2 (two states). Here, to distinguish groups, we also introduce eigenvalues for the cycling permutation operator $\begin{pmatrix} 123 \\ 231 \end{pmatrix} = (231)$, and its values are given as superscript to the corresponding wavefunctions.

$$\begin{aligned} I^{\text{tot}} = 3/2, \lambda = 1, \text{group } 1 \in A \\ \left| \frac{3}{2}, +\frac{3}{2} \right\rangle^1 &= |\alpha\alpha\alpha\rangle, \\ \left| \frac{3}{2}, +\frac{1}{2} \right\rangle^1 &= \frac{1}{\sqrt{3}}(|\alpha\alpha\beta\rangle + |\alpha\beta\alpha\rangle + |\beta\alpha\alpha\rangle), \\ \left| \frac{3}{2}, -\frac{1}{2} \right\rangle^1 &= \frac{1}{\sqrt{3}}(|\alpha\beta\beta\rangle + |\beta\alpha\beta\rangle + |\beta\beta\alpha\rangle) \\ \left| \frac{3}{2}, -\frac{3}{2} \right\rangle^1 &= |\beta\beta\beta\rangle, \\ I^{\text{tot}} = 1/2, \lambda = e^{i\frac{2\pi}{3}} = e^{+i\theta}, \text{group } 2 \in E_1 \\ \left| \frac{1}{2}, +\frac{1}{2} \right\rangle^{e^{+i\theta}} &= \frac{|\alpha\alpha\beta\rangle + e^{-i\theta}|\alpha\beta\alpha\rangle + e^{+i\theta}|\beta\alpha\alpha\rangle}{\sqrt{3}}, \\ \left| \frac{1}{2}, -\frac{1}{2} \right\rangle^{e^{+i\theta}} &= \frac{|\beta\beta\alpha\rangle + e^{-i\theta}|\beta\alpha\beta\rangle + e^{+i\theta}|\alpha\beta\beta\rangle}{\sqrt{3}}, \\ I^{\text{tot}} = 1/2, \lambda = e^{-i\frac{2\pi}{3}} = e^{-i\theta}, \text{group } 3 \in E_2 \\ \left| \frac{1}{2}, +\frac{1}{2} \right\rangle^{e^{-i\theta}} &= \frac{|\alpha\alpha\beta\rangle + e^{+i\theta}|\alpha\beta\alpha\rangle + e^{-i\theta}|\beta\alpha\alpha\rangle}{\sqrt{3}}, \\ \left| \frac{1}{2}, -\frac{1}{2} \right\rangle^{e^{-i\theta}} &= \frac{|\beta\beta\alpha\rangle + e^{+i\theta}|\beta\alpha\beta\rangle + e^{-i\theta}|\alpha\beta\beta\rangle}{\sqrt{3}}. \end{aligned} \tag{A6}$$

The C_3 permutation group $G = \left\{ \begin{pmatrix} 1 & 2 & 3 \\ 1 & 2 & 3 \end{pmatrix}, \begin{pmatrix} 1 & 2 & 3 \\ 2 & 3 & 1 \end{pmatrix}, \begin{pmatrix} 1 & 2 & 3 \\ 3 & 1 & 2 \end{pmatrix} \right\} = \{(), (+\theta), (-\theta)\}$ of the A_3 system consists of three permutations: The trivial identity permutation, permutation, or “+ θ ” rotation and “- θ ” rotation, with $\theta = \frac{2\pi}{3}$.

Table A2. Table of characters for A_3 three spin-1/2 system (C_3 group). Here $\theta = \frac{2\pi}{3}$. Note the difference between three different “E” here. The characters for spin representations (SpinRep) are filled using Equation (A4) and the following discussions. Any permutation (or rotation) will leave only states $|\alpha\alpha\alpha\rangle$ and $|\beta\beta\beta\rangle$ on the diagonal. This means that the sum of diagonal elements and corresponding character value is 2.

	E	C_3^1	C_3^2
A	1	1	1
E_1	1	$e^{i\theta}$	$e^{-i\theta}$
E_2	1	$e^{-i\theta}$	$e^{i\theta}$
SpinRep = $4A + 2E_1 + 2E_2$	8	2	2

Summarizing, there are four symmetric (g) states and two pairs of rotationally symmetric states ($E_i, |S\rangle$) states. It follows from both Equation (A6) and Table A2. Therefore, the basis for the A_3 three spin-1/2 system consists of three sets with multiplicities 4, 2, and 2 (SpinRep = $4A + 2E_1 + 2E_2$):

$$\begin{aligned}
 S_A^{123} &= \left\{ \left| \frac{3}{2}, +\frac{3}{2} \right\rangle^1, \left| \frac{3}{2}, +\frac{1}{2} \right\rangle^1, \left| \frac{3}{2}, -\frac{1}{2} \right\rangle^1, \left| \frac{3}{2}, -\frac{3}{2} \right\rangle^1 \right\}, \\
 S_{E_1}^{123} &= \left\{ \left| \frac{1}{2}, +\frac{1}{2} \right\rangle^{e^{+i\theta}}, \left| \frac{1}{2}, -\frac{1}{2} \right\rangle^{e^{+i\theta}} \right\}, \\
 S_{E_2}^{123} &= \left\{ \left| \frac{1}{2}, +\frac{1}{2} \right\rangle^{e^{-i\theta}}, \left| \frac{1}{2}, -\frac{1}{2} \right\rangle^{e^{-i\theta}} \right\}
 \end{aligned}
 \tag{A7}$$

Appendix A.3. A4 Four Spin-1/2 System: C4 Group Example

The number of states is $2^4 = 16$.

The basis of four spins can be grouped into four groups with total spin I^{tot} of 2 (five states), 1 (three groups, each consists of three states), and 0 (two groups, each with one state).

The C_4 permutation group $G = \left\{ \begin{pmatrix} 1 & 2 & 3 & 4 \\ 1 & 2 & 3 & 4 \end{pmatrix}, \begin{pmatrix} 1 & 2 & 3 & 4 \\ 2 & 3 & 4 & 1 \end{pmatrix}, \begin{pmatrix} 1 & 2 & 3 & 4 \\ 3 & 4 & 1 & 2 \end{pmatrix}, \begin{pmatrix} 1 & 2 & 3 & 4 \\ 4 & 1 & 2 & 3 \end{pmatrix} \right\} = \{(), (2341), (3412), (4123)\}$ of the A_4 system consists of four permutations: () Trivial identity permutation and three cyclic permutations that are equivalent to the rotation of a square by $90^\circ, 180^\circ,$ and 270° around the center axis perpendicular to its plane. Note that only 180° rotation can be represented as two consequent permutations $(3412) = (13)(24)$.

Table A3. Table of characters for A_4 four spin-1/2 system (C_4 group). The characters for SpinRep are filled using Equation (A4) and the following discussion. Any rotations will leave states $|\alpha\alpha\alpha\alpha\rangle$ and $|\beta\beta\beta\beta\rangle$ on diagonal. All other states change after an odd number of cyclic permutations. Hence, character for C_4 and $(C_4)^3$ is only 2. 180° rotation ((31)(42) permutation) also does not change $|\alpha\beta\alpha\beta\rangle$ and $|\beta\alpha\beta\alpha\rangle$ states. Hence, the corresponding character is $2 + 2 = 4$. This means that the sum of diagonal elements and corresponding character values are 4 for each rotation (permutation).

	E	C_4	$C_2 = (C_4)^2$	$(C_4)^3$
A	+1	+1	+1	+1
B	+1	-1	+1	-1
E_1	+1	+i	-1	-i
E_2	+1	-i	-1	+i
SpinRep = $6A + 4B + 3E_1 + 3E_2$	16	2	4	2

Appendix A.4. AA'(AA') Four Spin-1/2 System: D2 Group (Spin Symmetry of Ethylene)

The number of states is $2^4 = 16$.

The basis of four spins can be grouped into four groups with total spin I^{tot} of 2 (five states), 1 (three groups, each consists of three states), and 0 (two groups, each with one state).

The D_2 permutation group $G = \left\{ \begin{pmatrix} 1 & 2 & 3 & 4 \\ 1 & 2 & 3 & 4 \end{pmatrix}, \begin{pmatrix} 1 & 2 & 3 & 4 \\ 2 & 1 & 4 & 3 \end{pmatrix}, \begin{pmatrix} 1 & 2 & 3 & 4 \\ 3 & 4 & 1 & 2 \end{pmatrix}, \begin{pmatrix} 1 & 2 & 3 & 4 \\ 4 & 3 & 2 & 1 \end{pmatrix} \right\} = \{(), (21)(43), (31)(42), (41)(32)\}$ of the $AA'(AA')$ system consists of four permutations: $()$ – Trivial identity permutation and three pairwise permutations that are equivalent to rotations of the rectangle by 180° around three orthogonal axes, which are orthogonal to the plane of the rectangle and (or) its edges. We do not present the corresponding basis for a general D_2 group here, which is equivalent to D_{2h} discussed below.

Table A4. Table of characters for $AA'(AA')$ four spin-1/2 system (D_2 group). The characters for SpinRep are filled using Equation A4 and the following discussion. Any rotations will leave states $|\alpha\alpha\alpha\alpha$ and $|\beta\beta\beta\beta$ on diagonal. In addition, states $|\alpha\alpha\beta\beta$ and $|\beta\beta\alpha\alpha$ do not change by the action of (21)(43) permutation. For two other rotations, one can also write the corresponding two states. It means that the sum of diagonal elements and corresponding character values are 4 for each rotation (permutation).

	E	$C_2(z)$	$C_2(y)$	$C_2(x)$
A	+1	+1	+1	+1
B_1	+1	+1	−1	−1
B_2	+1	−1	+1	−1
B_3	+1	−1	−1	+1
SpinRep = 7A + 3 B_1 + 3 B_2 + 3 B_3	16	4	4	4

Appendix A.5. $AA'(AA')$ Four Spin-1/2 System, D_{2h} Group (Molecular Symmetry of Ethylene)

The number of states is $2^4 = 16$ [7].

The basis of four spins can be grouped into four groups with total spin I^{tot} of 2 (five states), 1 (three groups, each consists of three states), and 0 (two groups, each with one state).

The D_{2h} group is a direct product of D_2 and C_i groups. The D_2 part consists of four spin permutations $G(D_2) = \{(), (21)(43), (31)(42), (41)(32)\}$. The addition of the inversion operator of C_i results in four additional transformations $\{i, \sigma(xy), \sigma(xz), \sigma(yz)\}$: Inversion “I” and three mirror σ -planes: xy , xz , or yz (Figures 4 and A1).

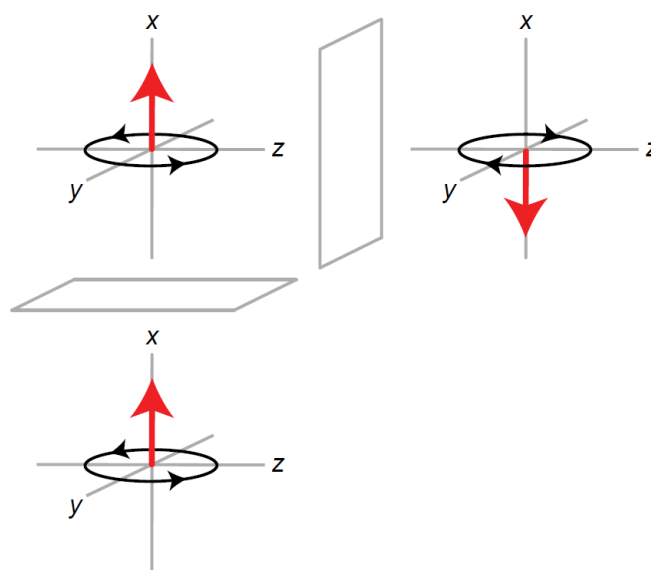


Figure A1. The action of a mirror plane on an axial vector (spin or magnetic dipole). When an axial vector is perpendicular to the mirror plane, it does not change upon reflection. If, however, it is oriented along the mirror plane, it changes its orientation upon reflection [63].

The eigenvectors for ethylene were found in [7] and are given in Equation (A8) without any changes.

$$\begin{aligned}
 I^{tot} = 2, \lambda = 1, \text{group } 1 \in A_g \\
 |2, +2\rangle^g &= |\alpha\alpha\alpha\alpha\rangle, \\
 |2, +1\rangle^g &= \frac{|\alpha\alpha\alpha\beta\rangle + |\alpha\alpha\beta\alpha\rangle + |\alpha\beta\alpha\alpha\rangle + |\beta\alpha\alpha\alpha\rangle}{2}, \\
 |2, 0\rangle^g &= \frac{|\alpha\alpha\beta\beta\rangle + |\alpha\beta\alpha\beta\rangle + |\alpha\beta\beta\alpha\rangle + |\beta\alpha\beta\alpha\rangle + |\beta\beta\alpha\alpha\rangle + |\beta\alpha\alpha\beta\rangle}{\sqrt{6}}, \\
 |2, -1\rangle^g &= \frac{|\beta\beta\beta\alpha\rangle + |\beta\beta\alpha\beta\rangle + |\beta\alpha\beta\beta\rangle + |\alpha\beta\beta\beta\rangle}{2}, \\
 |2, -2\rangle^g &= |\beta\beta\beta\beta\rangle, \\
 I^{tot} = 1, \text{group } 2 \in B_{1u} \\
 |1, +1\rangle^{1u} &= \frac{-|\alpha\alpha\alpha\beta\rangle - |\alpha\alpha\beta\alpha\rangle + |\alpha\beta\alpha\alpha\rangle + |\beta\alpha\alpha\alpha\rangle}{2}, \\
 |1, 0\rangle^{1u} &= \frac{|\alpha\alpha\beta\beta\rangle - |\beta\beta\alpha\alpha\rangle + \sqrt{2}}{2}, \\
 |1, -1\rangle^{1u} &= \frac{|\beta\beta\beta\alpha\rangle + |\beta\beta\alpha\beta\rangle - |\beta\alpha\beta\beta\rangle - |\alpha\beta\beta\beta\rangle}{2}, \\
 I^{tot} = 1, \text{group } 3 \in B_{2u} \\
 |1, +1\rangle^{2u} &= \frac{|\alpha\alpha\alpha\beta\rangle - |\alpha\alpha\beta\alpha\rangle + |\alpha\beta\alpha\alpha\rangle - |\beta\alpha\alpha\alpha\rangle}{2}, \\
 |1, 0\rangle^{2u} &= \frac{|\alpha\beta\alpha\beta\rangle - |\beta\alpha\beta\alpha\rangle}{\sqrt{2}}, \\
 |1, -1\rangle^{2u} &= \frac{-|\beta\beta\beta\alpha\rangle + |\beta\beta\alpha\beta\rangle - |\beta\alpha\beta\beta\rangle + |\alpha\beta\beta\beta\rangle}{2}, \\
 I^{tot} = 1, \text{group } 4 \in B_{3g} \\
 |1, +1\rangle^{3g} &= \frac{-|\alpha\alpha\alpha\beta\rangle + |\alpha\alpha\beta\alpha\rangle + |\alpha\beta\alpha\alpha\rangle - |\beta\alpha\alpha\alpha\rangle}{2}, \\
 |1, 0\rangle^{3g} &= \frac{|\beta\alpha\alpha\beta\rangle - |\alpha\beta\beta\alpha\rangle}{\sqrt{2}}, \\
 |1, -1\rangle^{3g} &= \frac{-|\beta\beta\beta\alpha\rangle + |\beta\beta\alpha\beta\rangle + |\beta\alpha\beta\beta\rangle - |\alpha\beta\beta\beta\rangle}{2}, \\
 I^{tot} = 0, \text{group } 5 \in A_g \\
 |0, 0\rangle^{g,s1} &= \frac{-\kappa|\beta\beta\alpha\alpha\rangle + |\beta\alpha\beta\alpha\rangle + (\kappa-1)|\beta\alpha\alpha\beta\rangle + (\kappa-1)|\alpha\beta\beta\alpha\rangle + |\alpha\beta\alpha\beta\rangle - \kappa|\alpha\alpha\beta\beta\rangle}{2\sqrt{1-\kappa+\kappa^2}}, \\
 I^{tot} = 0, \text{group } 6 \in A_g \\
 |0, 0\rangle^{g,s2} &= \frac{(\kappa-2)|\beta\beta\alpha\alpha\rangle - (2\kappa-1)|\beta\alpha\beta\alpha\rangle + (\kappa+1)|\beta\alpha\alpha\beta\rangle + (\kappa+1)|\alpha\beta\beta\alpha\rangle - (2\kappa-1)|\alpha\beta\alpha\beta\rangle + (\kappa-2)|\alpha\alpha\beta\beta\rangle}{2\sqrt{3}\sqrt{1-\kappa+\kappa^2}}. \\
 \text{with } \kappa &= \frac{\sqrt{J_s^2 + J_c^2 + J_t^2 - (J_s J_c + J_s J_t + J_c J_t)} + (J_s - J_c)}{J_s - J_t}
 \end{aligned} \tag{A8}$$

It is not as trivial as before to fill the SpinRep line in the character Table A5 as in the previous cases; this needs some elaboration. However, the first four elements are identical to the one from Table A4 for group D₂.

Let us consider the mirror plane $\sigma(yz)$ (Figure 1A), which also can be referred to as σ_h . It does not change the position of atoms (a), and because spin is an axial vector (b) the spin states do not change under the action of $\sigma(yz)$. Hence, the corresponding character is 16 (number of spin states). We refer to this operator as parity in the main text, and it changes the sign of one coordinate axis (here x).

Now, let us consider two mirror planes $\sigma(xy)$ and $\sigma(xz)$ (Figure 1A), also referred to as σ_v . σ_v exchanges two neighbor protons (permutations (21)(43) or (41)(32)) and changes the sign of the spin projection (it is not convenient for NMR, but using this notation of the axis, we assume the projections of the spin states along the x-axis). So, when two pairs of protons are exchanged and their sign is inverted, then there are only four states that do not change under the action of this transformation: $|\alpha\beta\alpha\beta\rangle$, $|\beta\alpha\alpha\beta\rangle$, $|\beta\alpha\beta\alpha\rangle$, and $|\alpha\beta\beta\alpha\rangle$ for the case of (21)(43) permutation with inversion. Four analogous states can be written for the other mirror transformation. Hence, the two corresponding characters are 4.

Finally, the inversion operator, i , exchanges the protons as (31)(42) (a) and changes the sign of the spin projections, meaning that only four states $|\alpha\alpha\beta\beta\rangle$, $|\beta\beta\alpha\alpha\rangle$, $|\beta\alpha\alpha\beta\rangle$, and $|\alpha\beta\beta\alpha\rangle$ will stay the same; hence, the corresponding character is 4.

Table A5. Table of characters for AA' (AA') four spin-1/2 system (D_{2h} group). This can be obtained as a direct product of C_i (the same as C₂) and D₂ character groups. See text for how to fill SpinRep line.

	E	C ₂ (z)	C ₂ (y)	C ₂ (x)	i	σ(xy)	σ(xz)	σ(yz)
A _g	+1	+1	+1	+1	+1	+1	+1	+1
B _{1g}	+1	+	−1	−1	+1	+1	−1	−1
B _{2g}	+1	−1	+1	−1	+1	−1	+1	−1
B _{3g}	+1	−1	−1	+1	+1	−1	−1	+1
A _u	+1	+1	+1	+1	−1	−1	−1	−1
B _{1u}	+1	+1	−1	−1	−1	−1	+1	+1
B _{2u}	+1	−1	+1	−1	−1	+1	−1	+1
B _{3u}	+1	−1	−1	+1	−1	+1	+1	−1
SpinRep = 7A _g + 3B _{1u} + 3B _{2u} + 3B _{3g}	16	4	4	4	4	4	4	16

There are seven symmetrical (A_g symmetry) states and three states for each of the three B symmetries (B_{1u}, B_{2u}, and B_{3g}). This follows from both Equation (A8) and Table A5. Therefore, the basis for the AA' (AA') four spin-1/2 system of D_{2h} symmetry consists of four sets with multiplicities of 7, 3, 3, and 3 (Spins rep. = 7A_g + 3B_{1u} + 3E_{2g} + 3E_{3u}):

$$\begin{aligned}
 S_{A_g}^{D_{2h}} &= \left\{ |2,+2\rangle^g, |2,+1\rangle^g, |2,0\rangle^g, |2,-1\rangle^g, |2,-2\rangle^g, |0,0\rangle^{g,s1}, |0,0\rangle^{g,s2} \right\}, \\
 S_{B_{1u}}^{D_{2h}} &= \left\{ |1,+1\rangle^{1u}, |1,0\rangle^{1u}, |1,-1\rangle^{1u} \right\}, \\
 S_{B_{2u}}^{D_{2h}} &= \left\{ |1,+1\rangle^{2u}, |1,0\rangle^{2u}, |1,-1\rangle^{2u} \right\}, \\
 S_{B_{3g}}^{D_{2h}} &= \left\{ |1,+1\rangle^{3g}, |1,0\rangle^{3g}, |1,-1\rangle^{3g} \right\}
 \end{aligned}
 \tag{A9}$$

Note that in the case of C₄ symmetry considered earlier, six states belong to the A_(g) group.

Appendix B

Table A6. Maximum expected polarization transfer coefficient ζ_{max} for systems without symmetry constraints and pH₂-derived spin order transfer (states σ_{ZZ}^{A,B} or σ_S^{A,B}) to the longitudinal polarization of all protons of the same molecule (average polarization).

Type of the System	Number of Spins	ζ _{max} from σ _{ZZ} ^{A,B} = ζσ _P ^X + σ _{rest}	ζ _{max} from σ _S ^{A,B} = ζσ _P ^X + σ _{rest}
AB	2	1/2	1
ABC	3	1/2	2/3
ABCD	4	3/8	5/8
ABCDE	5	3/8	11/20
ABCDEF	6	5/16	1/2
ABCDEFG	7	5/16	0.4821
ABCDEFGH	8	0.2734	0.4336
ABCDEFGHI	9	0.2734	0.4323
ABCDEFGHIJ	10	0.2461	0.3906
ABCDEFGHIJK	11	0.2461	0.3835
ABCDEFGHIJKL	12	0.2256	0.3597

Table A7. Maximum expected polarization transfer coefficient ζ_{\max}^{SC} for systems with symmetry constraints and pH₂-derived spin order transfer (state $\sigma_S^{A,B}$) to the longitudinal polarization of all protons of the same molecule (average polarization).

Type of the System	Number of Spins	ζ_{\max}^{SC} from $\sigma_S^{A,B} = \zeta \sigma_P^X + \sigma_{\text{rest}}$
A ₂ B	3	1/3
A ₂ BC	4	0.3125
A ₃ B	4	0.25
A ₂ B ₂	4	0.1875
A ₃ BC	5	0.175
A ₂ B ₂ C	5	0.175
A ₃ B ₂	5	0.1167
A ₃ BCD	6	0.2014
A ₃ B ₂ C	6	0.1424
A ₃ B ₃	6	0.1204

Appendix C

Here, we exemplify that more than 200% polarization per molecule is predicted in the absence of symmetry constraints for $N \geq 4$. We also investigate analytically asymptotic behavior for $N \gg 1$.

First, we will write down the eigenvalues of the target state σ_P^N (Equation (8)) for a different number of spins. Because the Zeeman basis is the eigenbasis of σ_P^N , the eigenvalues of σ_P^N are:

$$\Lambda^\uparrow(\sigma_P^N) = \frac{1}{2^{N-1}} [\text{Vector of ordered spin projections of Zeeman states}]$$

$$= \frac{1}{2^{N-1}} \left[\binom{N}{k} \text{ times } \left(-\frac{N}{2} + k\right) \right], \tag{A10}$$

where $\binom{N}{k}$ is the binomial coefficient and k is an integer number spanning from 0 to N .

Eigenvalues for $N = 2, 3$, and 4 are:

$$\Lambda^\uparrow(\sigma_P^{N=2}) = \frac{1}{2} [-1, 0, 0, 1],$$

$$\Lambda^\uparrow(\sigma_P^{N=3}) = \frac{1}{4} \left[-\frac{3}{2}, -\frac{1}{2}, -\frac{1}{2}, -\frac{1}{2}, \frac{1}{2}, \frac{1}{2}, \frac{1}{2}, \frac{3}{2}\right], \tag{A11}$$

$$\Lambda^\uparrow(\sigma_P^{N=4}) = \frac{1}{8} [-2, -1, -1, -1, -1, 0, 0, 0, 0, 0, 0, 1, 1, 1, 1, 2].$$

Second, we write down eigenvalues for the initial singlet spin order $\hat{\sigma}_S^{A,B|N}$ (Equation (1)):

$$\hat{\sigma}_S^{A,B|N} = \hat{\rho}_S^{A,B} - \frac{\hat{1}^N}{2^N} = -\frac{1}{2^{N-2}} \begin{pmatrix} \wedge^A & \wedge^B \\ \mathbf{I} & \cdot \mathbf{I} \end{pmatrix}. \tag{A12}$$

This operator is diagonal on the basis where the (S-T)-basis is used for A and B spins and the Zeeman basis is used for the rest of (N-2) spins, respectively. The general rule is as follows:

$$\Lambda^\uparrow(\hat{\sigma}_S^{A,B|N}) = \frac{1}{2^{N-2}} \left[(3 \times 2^{N-2}) \text{ times } \left(-\frac{1}{4}\right), \text{ and } (2^{N-2}) \text{ times } \left(\frac{3}{4}\right) \right]. \tag{A13}$$

This follows directly from the definition of $\hat{\rho}_S^{A,B}$ (Equation (1)) where one has 2^{N-2} times value $\left(\frac{1}{2^{N-2}}\right)$ and $3 \times 2^{N-2}$ times value 0 on the diagonal; this corresponds to the singlet state of A and B spins. The corresponding eigenvalues for $N = 2, 3$, and 4 are as follows:

$$\Lambda^\uparrow(\hat{\sigma}_S^{A,B|N=2}) = \frac{1}{4} [-1, -1, -1, 3],$$

$$\Lambda^\uparrow(\hat{\sigma}_S^{A,B|N=3}) = \frac{1}{8} [-1, -1, -1, -1, -1, -1, 3, 3], \tag{A14}$$

$$\Lambda^\uparrow(\hat{\sigma}_S^{A,B|N=4}) = \frac{1}{16} [12 \text{ times } (-1), 3, 3, 3, 3].$$

Now, using Equation (11) and eigenvalues of the target state (A13) and initial state (A16), one obtains the amplitude of the polarization transfer ξ^N :

$$\begin{aligned} \Lambda^\uparrow(\sigma_P^N=2) \cdot \Lambda^\uparrow(\sigma_P^N=2) &= \frac{1}{2}, \Lambda^\uparrow(\hat{\sigma}_S^{A,B|N=2}) \cdot \Lambda^\uparrow(\sigma_P^N=2) = \frac{1}{2}, \xi^{N=2} = 1, 2 \cdot \xi^{N=2} = 2 \\ \Lambda^\uparrow(\sigma_P^N=3) \cdot \Lambda^\uparrow(\sigma_P^N=3) &= \frac{3}{8}, \Lambda^\uparrow(\hat{\sigma}_S^{A,B|N=3}) \cdot \Lambda^\uparrow(\sigma_P^N=3) = \frac{1}{4}, \xi^{N=3} = \frac{2}{3}, 3 \cdot \xi^{N=3} = 2 \\ \Lambda^\uparrow(\sigma_P^N=4) \cdot \Lambda^\uparrow(\sigma_P^N=4) &= \frac{1}{4}, \Lambda^\uparrow(\hat{\sigma}_S^{A,B|N=4}) \cdot \Lambda^\uparrow(\sigma_P^N=4) = \frac{5}{32}, \xi^{N=4} = \frac{5}{8}, 4 \cdot \xi^{N=4} = 2.5 \end{aligned} \tag{A15}$$

It follows that average polarization decreases as the number of spins increases, but polarization per molecule increases and can exceed two units of 100% spin-1/2 polarization. This is illustrated in Figures 3 and 4.

For arbitrary N , one can use the known sums of binomial coefficients to find that

$$\begin{aligned} \Lambda^\uparrow(\sigma_P^N) \cdot \Lambda^\uparrow(\sigma_P^N) &= \frac{1}{2^{2N-2}} \sum_{k=0}^N \left(\frac{N^2}{4} - kN + k^2 \right) \binom{N}{k} \\ &= \frac{1}{2^{2N-2}} \left[\frac{N^2}{4} \sum_{k=0}^N \binom{N}{k} - N \sum_{k=0}^N k \binom{N}{k} + \sum_{k=0}^N k^2 \binom{N}{k} \right] \\ &= \frac{1}{2^{2N-2}} \left[\frac{N^2}{4} 2^N - N \cdot N \cdot 2^{N-1} + (N + N^2) \cdot 2^{N-2} \right] = \frac{N}{2^N}, \end{aligned} \tag{A16}$$

and

$$\Lambda^\uparrow(\hat{\sigma}_S^{A,B|N}) \cdot \Lambda^\uparrow(\sigma_P^N) = \frac{8 \cdot S}{2^{2N}}, \tag{A17}$$

where S is the sum of 2^{N-2} last elements in $\Lambda^\uparrow(\sigma_P^N)$. Note that 2^{N-2} is a quarter of all 2^N elements, and this will be important in the following evaluation. Then,

$$\xi^N = \frac{S}{2^{2N-3}} \cdot \frac{2^N}{N} = \frac{8 \cdot S}{N \cdot 2^N}. \tag{A18}$$

The explicit formula for calculating S is cumbersome:

$$S = \sum_{k=0}^{x_0} \left(\frac{N}{2} - k \right) \binom{N}{k} + \left(2^{N-2} - \sum_{k=0}^{x_0} \binom{N}{k} \right) \left(\frac{N}{2} - (x_0 + 1) \right) \tag{A19}$$

with x_0 defined such that the sum over binomial coefficients from 0 to x_0 does not exceed a quarter of all states (elements): $\sum_{k=0}^{x_0} \binom{N}{k} \leq 2^{N-2} \leq \sum_{k=0}^{x_0+1} \binom{N}{k}$. To the best of our knowledge, this expression does not have a simple solution; however, it can be simply calculated numerically. In the following, we derive an asymptotic solution for ξ^N when $N \gg 1$.

For the large N , the summation over binomial coefficients $\binom{N}{k}$ can be replaced by the integration over a normal distribution with a mean value of $N/2$ and variance $var = N/4$ (note that we use var for variance instead of conventional σ^2 to avoid confusion with spin operators):

$$\frac{1}{2^N} \sum_{k=0}^N [\times] \binom{N}{k} \approx \frac{1}{\sqrt{2\pi \cdot var}} \int_{-\infty}^{+\infty} [\times] e^{-\frac{(x-\frac{N}{2})^2}{2 \cdot var}} dx. \tag{A20}$$

Then, the value of S (Equations (A19) and (A21)) can be estimated as

$$\begin{aligned} S &\approx \frac{2^N}{\sqrt{2\pi \cdot var}} \int_{-\infty}^{x_0} \left(\frac{N}{2} - x'' \right) e^{-\frac{(\frac{N}{2}-x'')^2}{2 \cdot var}} dx'' = \frac{2^N}{\sqrt{2\pi \cdot var}} \int_{x_0}^{+\infty} x' e^{-\frac{x'^2}{2 \cdot var}} dx' \\ &= \frac{2^N \sqrt{var}}{\sqrt{2\pi}} \int_{x_0}^{+\infty} x e^{-\frac{x^2}{2}} dx = 2^N \sqrt{var} \cdot C = 2^{N-1} \sqrt{N} \cdot C. \end{aligned} \tag{A21}$$

where the value $C = \frac{1}{\sqrt{2\pi}} \int_{x_0}^{+\infty} x e^{-\frac{x^2}{2}} dx \cong 0.31(7)$ with $x_0 = 0.67448975$. This x_0 was found by solving an equation for the integral over the normal distribution equal to a quarter: $\frac{1}{\sqrt{2\pi}} \int_{x_0}^{+\infty} e^{-\frac{x^2}{2}} dx = 1/4$.

This is equivalent to a summation over a quarter of all elements in Equation (A21). Note that $\frac{1}{\sqrt{2\pi}} \int_{-\infty}^{+\infty} e^{-\frac{x^2}{2}} dx = 1$. Thus, for large N values, Equation (A19) is approximated as

$$\Lambda^\dagger(\hat{\sigma}_S^{A,B|N}) \cdot \Lambda^\dagger(\sigma_P^N) = \frac{8 \cdot S}{2^{2N}} \approx 4C \frac{\sqrt{N}}{2^N} \cong 1.271 \frac{\sqrt{N}}{2^N}. \quad (\text{A22})$$

Now we can find the maximum expected average polarization per spin ξ^N and per molecule $N \cdot \xi^N$ as

$$\xi^N \approx 4C \frac{\sqrt{N}}{2^N} \cdot \frac{2^N}{N} = \frac{4C}{\sqrt{N}} \cong \frac{1.271}{\sqrt{N}}; \quad N \cdot \xi^N \approx 4C \sqrt{N} \cong 1.271 \sqrt{N}. \quad (\text{A23})$$

This approximation (Equation (A23)) fits well the numerical simulations using Equations (A18) and (A19) and values for $N \leq 10$ demonstrated in the main manuscript (Figure 4).

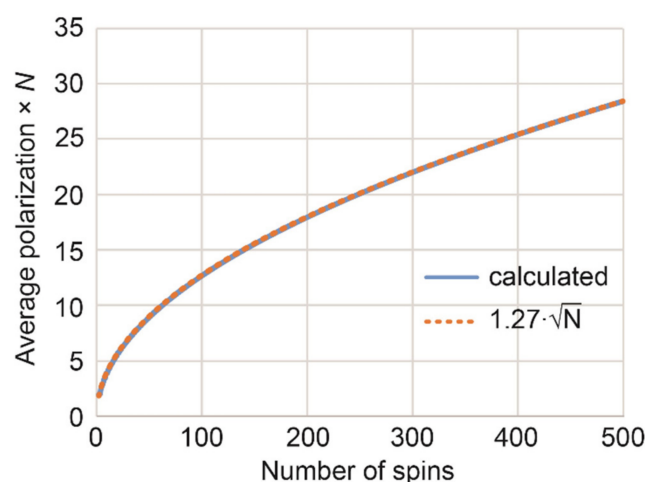


Figure A2. Average polarization per molecule—in units of one-spin-1/2 polarization—that can be achieved theoretically by adding pH₂ to a precursor producing a molecule with N spins without symmetry constraints. Numerically calculated values fit well to the approximation $1.271\sqrt{N}$.

References

- Natterer, J.; Bargon, J. Parahydrogen Induced Polarization. *Prog. Nucl. Magn. Reson. Spectrosc.* **1997**, *31*, 293–315. [\[CrossRef\]](#)
- Green, R.A.; Adams, R.W.; Duckett, S.B.; Mewis, R.E.; Williamson, D.C.; Green, G.G.R. The Theory and Practice of Hyperpolarization in Magnetic Resonance Using Parahydrogen. *Prog. Nucl. Magn. Reson. Spectrosc.* **2012**, *67*, 1–48. [\[CrossRef\]](#)
- Ellermann, F.; Pravdivtsev, A.; Hövener, J.-B. Open-Source, Partially 3D-Printed, High-Pressure (50-Bar) Liquid-Nitrogen-Cooled Parahydrogen Generator. *Magn. Reson.* **2021**, *2*, 49–62. [\[CrossRef\]](#)
- Hövener, J.-B.; Bär, S.; Leupold, J.; Jenne, K.; Leibfritz, D.; Hennig, J.; Duckett, S.B.; von Elverfeldt, D. A Continuous-Flow, High-Throughput, High-Pressure Parahydrogen Converter for Hyperpolarization in a Clinical Setting. *NMR Biomed.* **2013**, *26*, 124–131. [\[CrossRef\]](#)
- Feng, B.; Coffey, A.M.; Colon, R.D.; Chekmenev, E.Y.; Waddell, K.W. A Pulsed Injection Parahydrogen Generator and Techniques for Quantifying Enrichment. *J. Magn. Reson.* **2012**, *214*, 258–262. [\[CrossRef\]](#)
- Knopp, G.; Kirch, K.; Beaud, P.; Mishima, K.; Spitzer, H.; Radi, P.; Tulej, M.; Gerber, T. Determination of the Ortho-/Para Deuterium Concentration Ratio with Femtosecond CARS. *J. Raman Spectrosc.* **2003**, *34*, 989–993. [\[CrossRef\]](#)
- Zhivonitko, V.V.; Kovtunov, K.V.; Chapovsky, P.L.; Koptuyug, I.V. Nuclear Spin Isomers of Ethylene: Enrichment by Chemical Synthesis and Application for NMR Signal Enhancement. *Angew. Chem. Int. Ed.* **2013**, *52*, 13251–13255. [\[CrossRef\]](#)
- Kilaj, A.; Gao, H.; Rösch, D.; Rivero, U.; Küpper, J.; Willitsch, S. Observation of Different Reactivities of Para and Ortho- Water towards Trapped Diazenylium Ions. *Nat. Commun.* **2018**, *9*, 2096. [\[CrossRef\]](#)
- Bowers, C.R.; Weitekamp, D.P. Parahydrogen and Synthesis Allow Dramatically Enhanced Nuclear Alignment. *J. Am. Chem. Soc.* **1987**, *109*, 5541–5542. [\[CrossRef\]](#)
- Pravica, M.G.; Weitekamp, D.P. Net NMR Alignment by Adiabatic Transport of Parahydrogen Addition Products to High Magnetic Field. *Chem. Phys. Lett.* **1988**, *145*, 255–258. [\[CrossRef\]](#)
- Adams, R.W.; Aguilar, J.A.; Atkinson, K.D.; Cowley, M.J.; Elliott, P.I.P.; Duckett, S.B.; Green, G.G.R.; Khazal, I.G.; López-Serrano, J.; Williamson, D.C. Reversible Interactions with Para-Hydrogen Enhance NMR Sensitivity by Polarization Transfer. *Science* **2009**, *323*, 1708–1711. [\[CrossRef\]](#)

12. Korchak, S.; Mamone, S.; Glöggler, S. Over 50 % ¹H and ¹³C Polarization for Generating Hyperpolarized Metabolites—A Para-Hydrogen Approach. *ChemistryOpen* **2018**, *7*, 672–676. [[CrossRef](#)]
13. Hövener, J.-B.; Schwaderlapp, N.; Borowiak, R.; Lickert, T.; Duckett, S.B.; Mewis, R.E.; Adams, R.W.; Burns, M.J.; Highton, L.A.R.; Green, G.G.R.; et al. Toward Biocompatible Nuclear Hyperpolarization Using Signal Amplification by Reversible Exchange: Quantitative in Situ Spectroscopy and High-Field Imaging. *Anal. Chem.* **2014**, *86*, 1767–1774. [[CrossRef](#)]
14. Buckenmaier, K.; Scheffler, K.; Plaumann, M.; Fehling, P.; Bernarding, J.; Rudolph, M.; Back, C.; Koelle, D.; Kleiner, R.; Hövener, J.-B.; et al. Multiple Quantum Coherences Hyperpolarized at Ultra-Low Fields. *ChemPhysChem* **2019**, *20*, 2823–2829. [[CrossRef](#)]
15. Glöggler, S.; Müller, R.; Colell, J.; Emondts, M.; Dabrowski, M.; Blümich, B.; Appelt, S. Para-Hydrogen Induced Polarization of Amino Acids, Peptides and Deuterium–Hydrogen Gas. *Phys. Chem. Chem. Phys.* **2011**, *13*, 13759–13764. [[CrossRef](#)]
16. Barskiy, D.A.; Tayler, M.C.D.; Marco-Rius, I.; Kurhanewicz, J.; Vigneron, D.B.; Cikrikci, S.; Aydogdu, A.; Reh, M.; Pravdivtsev, A.N.; Hövener, J.-B.; et al. Zero-Field Nuclear Magnetic Resonance of Chemically Exchanging Systems. *Nat. Commun.* **2019**, *10*, 3002. [[CrossRef](#)]
17. Levitt, M.H. Symmetry Constraints on Spin Dynamics: Application to Hyperpolarized NMR. *J. Magn. Reson.* **2016**, *262*, 91–99. [[CrossRef](#)]
18. Ivanov, K.L.; Pravdivtsev, A.N.; Yurkovskaya, A.V.; Vieth, H.-M.; Kaptein, R. The Role of Level Anti-Crossings in Nuclear Spin Hyperpolarization. *Prog. Nucl. Magn. Reson. Spectrosc.* **2014**, *81*, 1–36. [[CrossRef](#)]
19. Bhattacharya, P.; Harris, K.; Lin, A.P.; Mansson, M.; Norton, V.A.; Perman, W.H.; Weitekamp, D.P.; Ross, B.D. Ultra-Fast Three Dimensional Imaging of Hyperpolarized ¹³C in Vivo. *Magn. Reson. Mater. Phys.* **2005**, *18*, 245–256. [[CrossRef](#)]
20. Schmidt, A.B.; Berner, S.; Braig, M.; Zimmermann, M.; Hennig, J.; von Elverfeldt, D.; Hövener, J.-B. In Vivo ¹³C-MRI Using SAMBADENA. *PLoS ONE* **2018**, *13*, e0200141. [[CrossRef](#)]
21. Svyatova, A.; Skovpin, I.V.; Chukanov, N.V.; Kovtunov, K.V.; Chekmenev, E.Y.; Pravdivtsev, A.N.; Hövener, J.-B.; Koptyug, I.V. ¹⁵N MRI of SLIC-SABRE Hyperpolarized ¹⁵N-Labelled Pyridine and Nicotinamide. *Chem. Eur. J.* **2019**, *25*, 8465–8470. [[CrossRef](#)]
22. Cavallari, E.; Carrera, C.; Aime, S.; Reineri, F. Metabolic Studies of Tumor Cells Using [1-¹³C] Pyruvate Hyperpolarized by Means of PHIP-Side Arm Hydrogenation. *ChemPhysChem* **2019**, *20*, 318–325. [[CrossRef](#)]
23. Sellies, L.; Aspers, R.; Feiters, M.C.; Rutjes, F.; Tessari, M. Para-Hydrogen Hyperpolarization Allows Direct NMR Detection of α -Amino Acids in Complex (Bio)Mixtures. *Angew. Chem. Int. Ed.* **2021**, *60*, 26954–26959. [[CrossRef](#)]
24. Nielsen, N.C.; Sorensen, O.W. Conditional Bounds on Polarization Transfer. *J. Magn. Reson. A* **1995**, *114*, 24–31. [[CrossRef](#)]
25. Nielsen, N.C.; Schulte-Herbrüggen, T.; Sørensen, O.W. Bounds on Spin Dynamics Tightened by Permutation Symmetry Application to Coherence Transfer in I2S and I3S Spin Systems. *Mol. Phys.* **1995**, *85*, 1205–1216. [[CrossRef](#)]
26. Sengstschmid, H.; Freeman, R.; Barkemeyer, J.; Bargon, J. A New Excitation Sequence to Observe the PASADENA Effect. *J. Magn. Reson. A* **1996**, *120*, 249–257. [[CrossRef](#)]
27. Kiryutin, A.S.; Ivanov, K.L.; Yurkovskaya, A.V.; Vieth, H.-M.; Lukzen, N.N. Manipulating Spin Hyper-Polarization by Means of Adiabatic Switching of a Spin-Locking RF-Field. *Phys. Chem. Chem. Phys.* **2013**, *15*, 14248–14255. [[CrossRef](#)]
28. Pravdivtsev, A.N.; Yurkovskaya, A.V.; Petrov, P.A.; Vieth, H.-M. Coherent Evolution of Singlet Spin States in PHOTO-PHIP and M2S Experiments. *Phys. Chem. Chem. Phys.* **2017**, *19*, 25961–25969. [[CrossRef](#)]
29. Pravdivtsev, A.N.; Kiryutin, A.S.; Yurkovskaya, A.V.; Vieth, H.-M.; Ivanov, K.L. Robust Conversion of Singlet Spin Order in Coupled Spin-1/2 Pairs by Adiabatically Ramped RF-Fields. *J. Magn. Reson.* **2016**, *273*, 56–64. [[CrossRef](#)]
30. Pravdivtsev, A.N.; Sönnichsen, F.; Hövener, J.-B. OnlyParahydrogen Spectroscopy (OPSY) Pulse Sequences—One Does Not Fit All. *J. Magn. Reson.* **2018**, *297*, 86–95. [[CrossRef](#)]
31. Aguilar, J.A.; Adams, R.W.; Duckett, S.B.; Green, G.G.R.; Kandiah, R. Selective Detection of Hyperpolarized NMR Signals Derived from Para-Hydrogen Using the Only Para-Hydrogen Spectroscopy (OPSY) Approach. *J. Magn. Reson.* **2011**, *208*, 49–57. [[CrossRef](#)]
32. Ratajczyk, T.; Gutmann, T.; Dillenberger, S.; Abdulhussaein, S.; Frydel, J.; Breitzke, H.; Bommerich, U.; Trantzschel, T.; Bernarding, J.; Magusin, P.C.M.M.; et al. Time Domain Para Hydrogen Induced Polarization. *Solid State Nucl. Magn. Reson.* **2012**, *43–44*, 14–21. [[CrossRef](#)]
33. Buntkowsky, G.; Gutmann, T.; Petrova, M.V.; Ivanov, K.L.; Bommerich, U.; Plaumann, M.; Bernarding, J. Dipolar Induced Para-Hydrogen-Induced Polarization. *Solid State Nucl. Magn. Reson.* **2014**, *63–64*, 20–29. [[CrossRef](#)]
34. Nasibulov, E.A.; Pravdivtsev, A.N.; Yurkovskaya, A.V.; Lukzen, N.N.; Vieth, H.-M.; Ivanov, K.L. Analysis of Nutation Patterns in Fourier-Transform NMR of Non-Thermally Polarized Multispin Systems. *Z. Phys. Chem.* **2013**, *227*, 929–953. [[CrossRef](#)]
35. Barskiy, D.A.; Salnikov, O.G.; Shchepin, R.V.; Feldman, M.A.; Coffey, A.M.; Kovtunov, K.V.; Koptyug, I.V.; Chekmenev, E.Y. NMR SLIC Sensing of Hydrogenation Reactions Using Parahydrogen in Low Magnetic Fields. *J. Phys. Chem. C* **2016**, *120*, 29098–29106. [[CrossRef](#)]
36. Vinogradov, E.; Grant, A.K. Hyperpolarized Long-Lived States in Solution NMR: Three-Spin Case Study in Low Field. *J. Magn. Reson.* **2008**, *194*, 46–57. [[CrossRef](#)]
37. Franzoni, M.B.; Buljubasich, L.; Spiess, H.W.; Münnemann, K. Long-Lived ¹H Singlet Spin States Originating from Para-Hydrogen in Cs-Symmetric Molecules Stored for Minutes in High Magnetic Fields. *J. Am. Chem. Soc.* **2012**, *134*, 10393–10396. [[CrossRef](#)]
38. Stevanato, G.; Roy, S.S.; Hill-Cousins, J.; Kuprov, I.; Brown, L.J.; Brown, R.C.D.; Pileio, G.; Levitt, M.H. Long-Lived Nuclear Spin States Far from Magnetic Equivalence. *Phys. Chem. Chem. Phys.* **2015**, *17*, 5913–5922. [[CrossRef](#)]
39. Grohmann, T.; Leibscher, M. Nuclear Spin Selective Alignment of Ethylene and Analogues. *J. Chem. Phys.* **2011**, *134*, 204316. [[CrossRef](#)]

40. Chapovsky, P.L.; Hermans, L.J.F. Nuclear Spin Conversion in Polyatomic Molecules. *Annu. Rev. Phys. Chem.* **1999**, *50*, 315–345. [[CrossRef](#)]
41. Chapovsky, P.L.; Zhivonitko, V.V.; Koptuyug, I.V. Conversion of Nuclear Spin Isomers of Ethylene. *J. Phys. Chem. A* **2013**, *117*, 9673–9683. [[CrossRef](#)]
42. San Fabián, J.; Casanueva, J.; Díez, E.; Esteban, A.L. Spin–Spin Coupling Constants in Ethylene: Equilibrium Values. *Chem. Phys. Lett.* **2002**, *361*, 159–168. [[CrossRef](#)]
43. Kaski, J.; Lantto, P.; Vaara, J.; Jokisaari, J. Experimental and Theoretical Ab Initio Study of the ^{13}C – ^{13}C Spin–Spin Coupling and ^1H and ^{13}C Shielding Tensors in Ethane, Ethene, and Ethyne. *J. Am. Chem. Soc.* **1998**, *120*, 3993–4005. [[CrossRef](#)]
44. Carrington, A.; McLachlan, A.D. *Introduction to Magnetic Resonance with Applications to Chemistry and Chemical Physics*; Harper & Row: New York, NY, USA, 1967.
45. DeVience, S.J.; Walsworth, R.L.; Rosen, M.S. Preparation of Nuclear Spin Singlet States Using Spin-Lock Induced Crossing. *Phys. Rev. Lett.* **2013**, *111*, 173002. [[CrossRef](#)]
46. Cavallari, E.; Carrera, C.; Boi, T.; Aime, S.; Reineri, F. Effects of Magnetic Field Cycle on the Polarization Transfer from Parahydrogen to Heteronuclei through Long-Range J-Couplings. *J. Phys. Chem. B* **2015**, *119*, 10035–10041. [[CrossRef](#)]
47. Schmidt, A.B.; Berner, S.; Schimpf, W.; Müller, C.; Lickert, T.; Schwaderlapp, N.; Knecht, S.; Skinner, J.G.; Dost, A.; Rovedo, P.; et al. Liquid-State Carbon-13 Hyperpolarization Generated in an MRI System for Fast Imaging. *Nat. Commun.* **2017**, *8*, ncomms14535. [[CrossRef](#)]
48. Cavallari, E.; Carrera, C.; Sorge, M.; Bonne, G.; Muchir, A.; Aime, S.; Reineri, F. The ^{13}C Hyperpolarized Pyruvate Generated by ParaHydrogen Detects the Response of the Heart to Altered Metabolism in Real Time. *Sci. Rep.* **2018**, *8*, 8366. [[CrossRef](#)]
49. Kovtunov, K.V.; Pokochueva, E.; Salnikov, O.; Cousin, S.; Kurzbach, D.; Vuichoud, B.; Jannin, S.; Chekmenev, E.; Goodson, B.; Barskiy, D.; et al. Hyperpolarized NMR: D-DNP, PHIP, and SABRE. *Chem. Asian J.* **2018**, *13*, 1857–1871. [[CrossRef](#)]
50. Lee, W.T.; Zheng, G.; Talbot, C.L.; Tong, X.; D’Adam, T.; Parnell, S.R.; Veer, M.D.; Jenkin, G.; Polglase, G.R.; Hooper, S.B.; et al. Hyperpolarised Gas Filling Station for Medical Imaging Using Polarised ^{129}Xe and ^3He . *Magn. Reson. Imag.* **2021**. [[CrossRef](#)]
51. Reineri, F.; Viale, A.; Ellena, S.; Boi, T.; Daniele, V.; Gobetto, R.; Aime, S. Use of Labile Precursors for the Generation of Hyperpolarized Molecules from Hydrogenation with Parahydrogen and Aqueous-Phase Extraction. *Angew. Chem. Int. Ed.* **2011**, *50*, 7350–7353. [[CrossRef](#)]
52. Chukanov, N.V.; Salnikov, O.G.; Shchepin, R.V.; Kovtunov, K.V.; Koptuyug, I.V.; Chekmenev, E.Y. Synthesis of Unsaturated Precursors for Parahydrogen-Induced Polarization and Molecular Imaging of 1- ^{13}C -Acetates and 1- ^{13}C -Pyruvates via Side Arm Hydrogenation. *ACS Omega* **2018**, *3*, 6673–6682. [[CrossRef](#)]
53. Nelson, S.J.; Kurhanewicz, J.; Vigneron, D.B.; Larson, P.E.Z.; Harzstark, A.L.; Ferrone, M.; van Criekinge, M.; Chang, J.W.; Bok, R.; Park, I.; et al. Metabolic Imaging of Patients with Prostate Cancer Using Hyperpolarized [1- ^{13}C]Pyruvate. *Sci. Transl. Med.* **2013**, *5*, 198ra108. [[CrossRef](#)]
54. Cunningham, C.H.; Lau, J.Y.C.; Chen, A.P.; Geraghty, B.J.; Perks, W.J.; Roifman, I.; Wright, G.A.; Connelly, K.A. Hyperpolarized ^{13}C Metabolic MRI of the Human Heart. *Circ. Res.* **2016**, *119*, 1177–1182.
55. Berner, S.; Schmidt, A.B.; Zimmermann, M.; Pravdivtsev, A.N.; Glöggler, S.; Hennig, J.; von Elverfeldt, D.; Hövener, J.-B. SAMBADENA Hyperpolarization of ^{13}C -Succinate in an MRI: Singlet-Triplet Mixing Causes Polarization Loss. *ChemistryOpen* **2019**, *8*, 728–736. [[CrossRef](#)]
56. Schmidt, A.B.; Brahms, A.; Ellermann, F.; Knecht, S.; Berner, S.; Hennig, J.; von Elverfeldt, D.; Herges, R.; Hövener, J.-B.; Pravdivtsev, A. Selective Excitation of Hydrogen Doubles the Yield and Improves the Robustness of Parahydrogen-Induced Polarization of Low- γ Nuclei. *Phys. Chem. Chem. Phys.* **2021**, *23*, 26645–26652. [[CrossRef](#)]
57. Olsson, L.E.; Chai, C.-M.; Axelsson, O.; Karlsson, M.; Golman, K.; Petersson, J.S. MR Coronary Angiography in Pigs with Intraarterial Injections of a Hyperpolarized ^{13}C Substance. *Magn. Reson. Med.* **2006**, *55*, 731–737. [[CrossRef](#)]
58. Pravdivtsev, A.; Brahms, A.; Kienitz, S.; Sönnichsen, F.D.; Hövener, J.-B.; Herges, R. Catalytic Hydrogenation of Trivinyl Orthoacetate: Mechanisms Elucidated by Parahydrogen Induced Polarization. *ChemPhysChem* **2021**, *22*, 370–377. [[CrossRef](#)]
59. Pravdivtsev, A.N.; Yurkovskaya, A.V.; Lukzen, N.N.; Ivanov, K.L.; Vieth, H.-M. Highly Efficient Polarization of Spin-1/2 Insensitive NMR Nuclei by Adiabatic Passage through Level Anticrossings. *J. Phys. Chem. Lett.* **2014**, *5*, 3421–3426. [[CrossRef](#)]
60. Knecht, S.; Blanchard, J.W.; Barskiy, D.; Cavallari, E.; Dagys, L.; Dyke, E.V.; Tsukanov, M.; Bliemel, B.; Münnemann, K.; Aime, S.; et al. Rapid Hyperpolarization and Purification of the Metabolite Fumarate in Aqueous Solution. *Proc. Natl. Acad. Sci.* **2021**, *118*. [[CrossRef](#)]
61. Eills, J.; Cavallari, E.; Kircher, R.; Matteo, G.D.; Carrera, C.; Dagys, L.; Levitt, M.H.; Ivanov, K.L.; Aime, S.; Reineri, F.; et al. Singlet-Contrast Magnetic Resonance Imaging: Unlocking Hyperpolarization with Metabolism. *Angew. Chem. Int. Ed.* **2021**, *60*, 6791–6798. [[CrossRef](#)]
62. Pravdivtsev, A.N.; Hövener, J.-B. Simulating Non-Linear Chemical and Physical (CAP) Dynamics of Signal Amplification By Reversible Exchange (SABRE). *Chem. Eur. J.* **2019**, *25*, 7659–7668. [[CrossRef](#)]
63. Rodríguez-Carvajal, J.; Bourée, F. Symmetry and Magnetic Structures. *EPJ Web Conf.* **2012**, *22*, 00010. [[CrossRef](#)]